

**This item is the archived peer-reviewed author-version of:**

Synthesis and evaluation of novel benzotropolones as Atg4B inhibiting autophagy blockers

**Reference:**

Tanc Muhammet, Cleenewerck Matthias, Kurdi Ammar, Roelandt Ria, Declercq Wim, De Meyer Guido, Augustyns Koen, Martinet Wim, van der Veken Pieter.-  
Synthesis and evaluation of novel benzotropolones as Atg4B inhibiting autophagy blockers  
Bioorganic chemistry - ISSN 0045-2068 - 87(2019), p. 163-168  
Full text (Publisher's DOI): <https://doi.org/10.1016/J.BIOORG.2019.03.021>  
To cite this reference: <https://hdl.handle.net/10067/1579250151162165141>

## Synthesis and evaluation of novel benzotropolones as Atg4B inhibiting autophagy blockers.

Muhammet Tanc,<sup>a‡</sup> Matthias Cleenewerck,<sup>a‡</sup> Ammar Kurdi,<sup>b</sup> Ria Roelandt,<sup>c, d</sup> Wim Declercq,<sup>c, d</sup> Guido De Meyer,<sup>b</sup> Koen Augustyns,<sup>a</sup> Wim Martinet,<sup>b\*</sup> Pieter van der Veken.<sup>a\*</sup>

<sup>a</sup> Laboratory of Medicinal Chemistry (UAMC), Department of Pharmaceutical Sciences, University of Antwerp, Antwerp, Belgium

<sup>b</sup>Laboratory of Physiopharmacology, Department of Pharmaceutical Sciences, University of Antwerp, Antwerp, Belgium

<sup>c</sup>VIB Inflammation Research Center, Technologiepark 927, B-9052, Ghent, Belgium

<sup>d</sup>Department of Biomedical Molecular Biology, Ghent University, Technologiepark 927, B-9052, Ghent, Belgium

### Abstract:

Autophagy is an intracellular degradation/recycling pathway that provides nutrients and building blocks to cellular metabolism and keeps the cytoplasm clear of obsolete proteins and organelles. During recent years, dysregulated autophagy activity has been reported to be a characteristic of many different disease types, including cancer and neurodegenerative disorders. This has created a strong case for development of autophagy modulating compounds as potential treatments for these diseases. Inhibitors of autophagy have been proposed as a therapeutic intervention in, *e.g.*, advanced cancer, and inhibiting the cysteine protease Atg4B has been put forward as a main strategy to block autophagy. We recently identified and demonstrated -both *in vitro* and *in vivo* - that compounds with a benzotropolone basic structure targeting Atg4B, can significantly slow down tumor growth and potentiate the effect of classical chemotherapy. In this study we report the synthesis and inhibition profile of new benzotropolone derivatives with additional structural modifications at 6 different positions. To obtain a solid inhibition profile, all compounds were evaluated on three levels, including two cell-based assays to confirm autophagy and intracellular Atg4B inhibition and an SDS-PAGE-based experiment to assess *in vitro* Atg4B affinity. Several molecules with a promising profile were identified.

**Keywords** : Autophagy, Atg4B, Benzotropolone, UAMC-2526

---

\*Corresponding authors. E-mail: [pieter.vanderveken@uantwerpen.be](mailto:pieter.vanderveken@uantwerpen.be) (P. Van der Veken) ; [wim.martinet@uantwerpen.be](mailto:wim.martinet@uantwerpen.be) (W. Martinet)

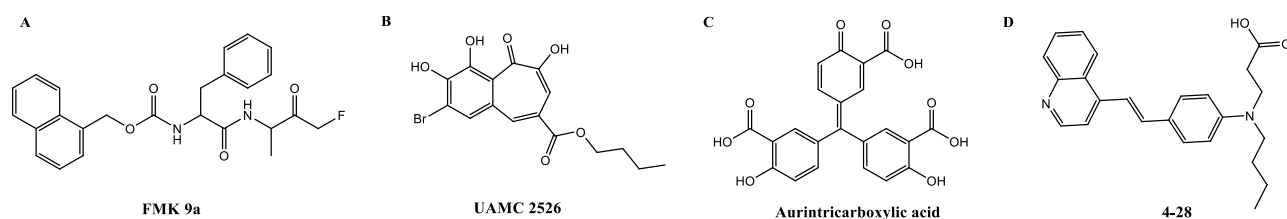
‡ Authors contributed equally.

## 1. Introduction

Autophagy is an intracellular recycling/degradation process that is remarkably evolutionary conserved from yeast to higher eukaryotes. It targets long-lived cytosolic proteins and organelles to subsidise cellular homeostasis and has also been demonstrated to be involved in host-pathogen interactions with viruses, bacteria and parasitic protozoa [1,2]. The process is characterized by the formation of double walled membrane vesicles called autophagosomes that engulf obsolete proteins and cellular components. Breakdown of the contents is ensured by fusing of autophagosomes with a lysosome. Autophagy is typically induced as a response to different stressors such as starvation or hypoxia [3]. In addition, dysregulated autophagy (i.e., either defective or upregulated autophagy) has recently been identified as a hallmark of multiple human disease types, including cancer, neurodegenerative disorders and cardiovascular disease [4]. As a consequence, there is a strong and growing demand for autophagy modulating compounds, both as research tools and as potential drugs. Inhibitors of autophagy can be expected to find main applications in oncology: it has been convincingly shown that cancer cells in advanced tumors draw heavily on autophagy to survive in the harsh conditions of the tumor micro environment. Furthermore, autophagy is known to protect cancer cells against oncolytic drugs by effectively limiting exchange of materials with the extracellular environment. [5,6].

To date, both direct and indirect strategies to block autophagy have been reported. Exemplary for the indirect approaches, lysosomal inhibitors like chloroquine and its derivatives have shown efficacy in a number of animal oncology models, and several clinical trials have meanwhile been initiated. Nonetheless, chloroquine derivatives and other molecules with similar activity (*e.g.*, bafilomycin) most likely only interfere with lysosomal acidification and do not have direct effects on the cell's autophagy machinery. In addition, the extracellular matrix acidification that is present in many advanced tumors, has been claimed to render chloroquine clinically inefficient [7]. Conversely, direct targeting of proteins involved in the autophagy cascade has been proposed as a potentially more interesting alternative. In this framework, Atg4B has several attractive features as a potential target for directly blocking autophagy. Atg4B is an enzyme with two well-defined activity types that have key roles during autophagosome formation and maturation. Both activity types are catalyzed by the same active center. First, Atg4B proteolytically primes its substrate LC3B relying on cysteine-type protease activity and generating LC3B-I. Further downstream in the autophagy cascade, LC3B-I is lipidated with phosphatidylethanolamine, yielding LC3B-II. The latter is essential for anchoring the so-called isolation membrane during autophagosome formation. Afterwards, Atg4B recycles LC3B-I by delipidating LC3B-II. In spite of significant effort by multiple groups, targeting Atg4B activity has so far proven daunting. Inhibitor discovery has been hindered by two factors. 1) First, the conformational dynamics of Atg4B in solution remain uncharacterized. Crystal structures have shown that the enzyme can adopt at least two conformations: an active ('open') and a putatively catalytically inert ('closed') form, each with distinct

pocket structures in the active center [8]. It is currently unclear whether the solution structure of Atg4B indeed corresponds to the closed conformation. 2) In addition, developing a straightforward and reliable Atg4B-activity assay to support inhibitor screening has been shown to be challenging. A readily accessible, standardized Atg4B-assay would also be most useful to compare, and benchmark reported Atg4B-inhibitory potencies of compounds. So far, both rational design strategies and several types of high throughput screening have only delivered compounds with affinities in the micromolar range. Remarkably, none of the compounds identified possess a typical, druglike ‘decorated scaffold’ architecture (**Figure 1**). Additionally, Roche’s fluoromethyl ketone FMK 9a was shown later to phenotypically induce autophagy (instead of inhibiting the process) [9-11]. Our own effort in this domain has been focusing on benzotropolone-derived molecules. Apparent Atg4B-affinities in an SDS-page based assay (*vide infra*) are typically also in the micromolar range, but these molecules nonetheless strongly suppress both Atg4B activity and autophagy *in cellulo* at 10  $\mu$ M concentrations. In addition, we have demonstrated that compound UAMC-2526 is capable of potently inhibiting autophagy *in vivo* and significantly reduces tumor growth in a HT29-mouse model of colorectal cancer. Notably, UAMC-2526 also significantly potentiates the effect of the reference chemotherapeutic oxaliplatin [12,13]. This study reports the synthesis and evaluation of 29 novel benzotropolone derivatives. It aims to provide a more profound insight in the Structure-Activity Relationship compound class, a topic which so far, we investigated superficially.



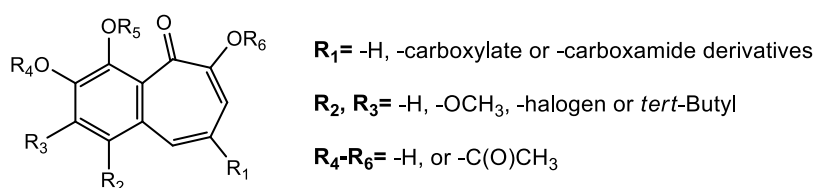
**Figure 1: Relevant examples of reported, Atg4B-targeting autophagy inhibitors (A) FMK 9a [14], (B) UAMC 2526 [13], (C) aurintricarboxylic acid [15], (D:) compound 4-28 [10].**

## 2. Results and Discussion

### 2.1 Chemistry

The generic benzotropolone structure covering all the new compounds in the manuscript has six variable positions ( $R_1$ - $R_6$ ) and is shown in **Figure 2**. A first aim of this study was to investigate the impact of the  $R^1$  substituent. Specifically, we were interested whether UAMC 2526’s butyl ester function at this position can be removed or replaced by a potentially more metabolically stable carboxamide group. Earlier preliminary work from us had indicated that the amide alternative could be worth investigating in more depth. [13] Likewise, we wanted to obtain more insight in the scope of *O*- or *N*- alkyl substituents that are tolerated at this position. In addition, we aimed to explore the effect of *O*- or *N*- alkyl substituents that are tolerated at this position. In addition, we aimed to explore the effect of halogenation at position  $R_2$ . Halogenation was considered interesting, since it has the potential to increase overall lipophilicity

and, possibly, cellular permeability. Reference UAMC 2526 already carries an R<sub>3</sub>-bromine group and while earlier work had shown this to be preferable over an R<sub>3</sub> fluorine or methoxy substituent in terms of cellular potency, open questions remained regarding the halogenation of the R<sub>2</sub>-position [13]. In the same framework, we decided to evaluate the introduction of an R<sub>2</sub>-methoxy and *tert*-butyl group. At the R<sub>4</sub>-R<sub>6</sub> positions, the compounds in this study in most cases carry a hydrogen atom. This is again based on the foregoing manuscript where it was shown that the phenol and enol-type alcohol functions of the benzotropolone basic skeleton are essential for autophagy blocking activity. Three compounds in the series nonetheless are derivatized with acetyl groups at these positions. The latter molecules were included as potential ester prodrugs that could have increased cellular permeability.

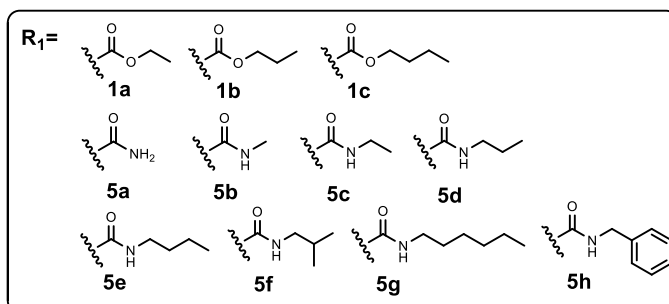
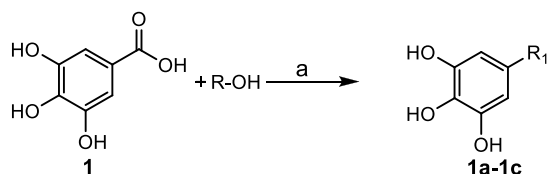


**Figure 2:** Overview of compounds prepared for this study.

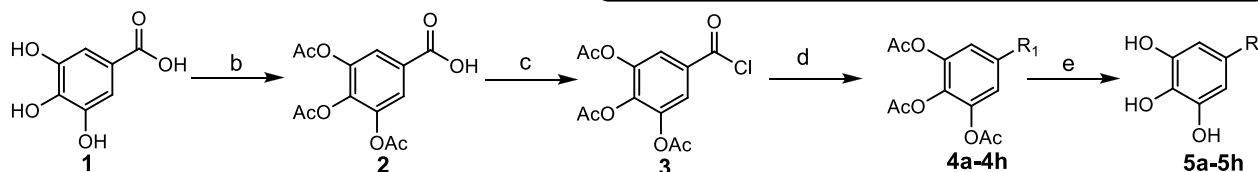
Noteworthy, the choice of substituents was also governed by their compatibility with the benzotropolone condensation reaction required for construction of all final products. The latter consists of a KIO<sub>3</sub>-mediated oxidative reaction of a gallic acid derivative and a catechol derivative (*vide infra*). Practically, the synthesis of the target molecules was initiated with the preparation of the gallic acid building blocks. The carboxylate function in these gallate building blocks corresponds to the R<sub>1</sub>-carboxylate group of the benzotropolone target compounds. (**Scheme 1, Entry A**). The required gallate esters (**1a-1c**), were obtained via Fisher-type, acid-catalyzed reaction between free gallic acid and one of the selected alcohols. Synthesis of the gallic acid amides, **5a - 5h**, was initiated by acetylation of **1** using acetic anhydride and a catalytic amount of H<sub>2</sub>SO<sub>4</sub> to yield the protected 3,4,5-triacetoxybenzoic acid **2**. The free carboxylate function of **2** was then converted to acyl chloride **3** using thionyl chloride. In the following step, a selected amine was added to obtain the protected amides **4a - 4h**. Deacetylation with hydrazine afforded the corresponding gallamides **5a - 5h**.

## A) Synthetic preparation of gallate building blocks:

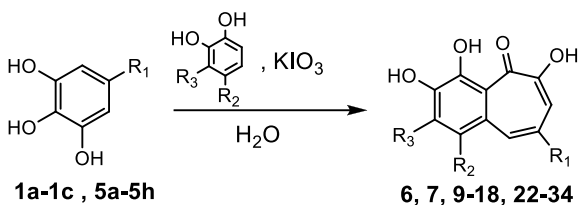
### 1) Gallic acid esters:



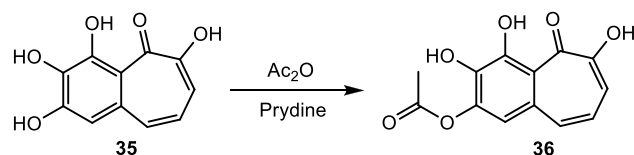
### 2) Gallic acid amides:



## B) Benzotropolone condensation



## C) Acetylation of 35



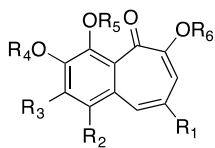
**Scheme 1:** Synthetic preparation of gallic acid-based intermediates (**Entry A**); final products (**Entry B**); and synthesis of compound **36** (**Entry C**). Reagents and conditions: (a) Alcohol, H<sub>2</sub>SO<sub>4</sub> (cat.), reflux, overnight (b) Ac<sub>2</sub>O, H<sub>2</sub>SO<sub>4</sub> (cat.), 80°C, 15'; (c) Dry toluene, SOCl<sub>2</sub>, reflux, 1.5h; (d) Amine, dry DCM, DIPEA, rt, 1h; (e) ACN, NH<sub>2</sub>NH<sub>2</sub>.H<sub>2</sub>O, rt, 0.5 h.

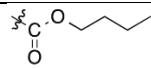
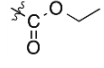
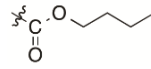
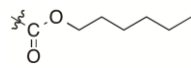
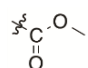
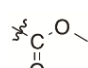
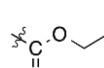
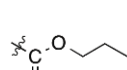
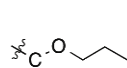
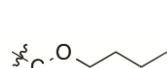
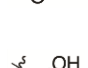

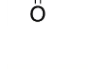
Compounds **8** and **35** were purchased from Sigma-Aldrich. Compound **19** was derived from methyl 3,4,6-trihydroxy-5-oxo-5H-benzo[7]annulene-8-carboxylate [**13**] via acetylation of the R<sub>4</sub>- R<sub>6</sub> positions by using acetic anhydride in basic conditions. The same synthetic strategy was used to obtain compound **20** from 3,4,6-trihydroxy-5-oxo-5H-benzo[7]annulene-8-carboxylic acid [**13**]. Compound **21** was derived from methyl 3,4,6-trihydroxy-5-oxo-5H-benzo[7]annulene-8-carboxylate [**13**] using ammonia in MeOH.

## 2.2. Compound evaluation.

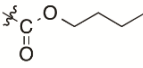
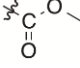
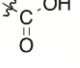
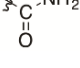
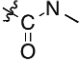
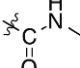
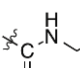
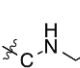
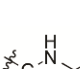
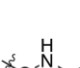
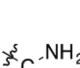
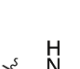
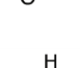
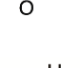
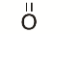
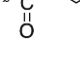
All compounds were evaluated on 3 complementary levels (**Table 1**). 1) First, a luciferase reporter assay reported by Ketteler was implemented for assessment of intracellular Atg4B inhibition. [16] HEK293 cells transfected with a [*Gaussia* luciferase- $\beta$ -actine-LC3] construct and treated with autophagy-inducing everolimus, are incubated with an autophagy inhibitor at 10 $\mu$ M concentration. Luminescence quantification is used as a measure of intracellular Atg4B inhibition. The lower a compound scores in this assay, the stronger it suppresses cellular Atg4B activity. In addition, the luminescence scores in **Table 1** are normalized, with luminescence in everolimus-treated controls equated to 1. 2) Second, inhibition of everolimus-induced autophagy in Jurkat cells (10  $\mu$ M inhibitor concentration) was used as a phenotypical screen to assess autophagy blocking potential. Read-out in this assay, published earlier by Stankov, consists of FACS-based fluorescence quantification of autophagy vacuoles in cells after treatment with the fluorescent CytoID reagent. Scores represented in **Table 1** represent the mean fluorescence intensities (based on 10.000 individual cell measurements/compound). In this assay, lower scores represent lower autophagosome fluorescence and, hence, stronger autophagy inhibition. Scores have also been normalized: fluorescence in everolimus-treated controls was equated to 1. Non-everolimus treated controls had a mean fluorescence score of 0.37. 3) Third, a previously published gel-based assay was used for Atg4B inhibitory potency determination [12]. The latter determines the % inhibition (500  $\mu$ M compound concentration) of Atg4B-mediated processing of LC3-GST, a fusion protein between LC3 and glutathione-S-transferase (GST). The read-out in this assay consists of densitometric quantification of remaining LC3-GST, separated from the other assay components using SDS-PAGE. Earlier benchmarking effort with literature Atg4B inhibitors has shown that the experimental parameters of this assay (e.g., the high enzyme and substrate concentrations required for reliable densitometric quantification) produce IC<sub>50</sub>-values that are systematically higher than in other reported assays. Compounds therefore appear to be less potent than they would in assay types where lower enzyme and substrate concentrations can be used. [14] We nonetheless also include results for the new compounds in the gel-based assay for the sake of completeness.

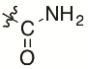


**Table 1: Screening results of the benzotropolone library.**



Compound	R <sub>1</sub>	R <sub>2</sub>	R <sub>3</sub>	R <sub>4</sub>	R <sub>5</sub>	R <sub>6</sub>	Luciferase reporter assay <sup>(a)</sup>	CYTO-ID assay <sup>(b)</sup>	% Atg4B inhibition
<b>3-MA<sup>(c)</sup></b>							N.D. <sup>(d)</sup>	<b>0.57</b>	N.D.
<b>UAMC-2526<sup>(e)</sup></b>		H	Br	H	H	H	<b>0.43</b>	<b>0.55</b>	<b>49.97</b>
<b>6</b>		H	H	H	H	H	<b>0.89</b>	<b>0.76</b>	<b>42.25</b>
<b>7</b>		H	OCH <sub>3</sub>	H	H	H	N.D. <sup>(e)</sup>	N.D.	<b>9.67</b>
<b>8</b>		H	OCH <sub>3</sub>	H	H	H	<b>0.67</b>	<b>0.46</b>	<b>19.79</b>
<b>9</b>		H	OCOCH <sub>3</sub>	H	H	H	N.D.	<b>1.01</b>	<b>0.00</b>
<b>10</b>		H	Br	H	H	H	<b>0.67</b>	<b>0.99</b>	<b>30.30</b>
<b>11</b>		H	Br	H	H	H	<b>0.85</b>	<b>0.94</b>	<b>16.69</b>
<b>12</b>		H	Br	H	H	H	<b>0.17</b>	<b>0.52</b>	<b>18.03</b>
<b>13</b>		H	Cl	H	H	H	<b>0.24</b>	<b>0.35</b>	<b>24.66</b>
<b>14</b>		H	Cl	H	H	H	N.D.	<b>1.26</b>	<b>54.45</b>
<b>15</b>		OCH <sub>3</sub>	H	H	H	H	N.D.	<b>0.93</b>	<b>30.59</b>
<b>16</b>		Cl	H	H	H	H	<b>0.18</b>	<b>0.29</b>	<b>12.46</b>
<b>17</b>		C(CH <sub>3</sub> ) <sub>3</sub>	H	H	H	H	<b>0.44</b>	<b>0.60</b>	<b>2.62</b>



18		C(CH <sub>3</sub> ) <sub>3</sub>	H	H	H	H	0.54	0.86	3.86
19		H	H	COCH <sub>3</sub>	COCH <sub>3</sub>	COCH <sub>3</sub>	1.02	N.D.	13.00
20		H	H	COCH <sub>3</sub>	COCH <sub>3</sub>	COCH <sub>3</sub>	0.87	N.D.	11.57
21		H	H	H	H	H	0.82	0.53	63.83
22		H	H	H	H	H	0.96	0.90	47.71
23		H	H	H	H	H	0.62	1.10	67.34
24		H	H	H	H	H	0.46	1.01	68.75
25		H	H	H	H	H	0.18	0.98	31.88
26		H	H	H	H	H	0.27	0.62	67.95
27		H	H	H	H	H	0.16	0.91	28.09
28		H	Br	H	H	H	0.75	0.85	63.28
29		H	Br	H	H	H	0.18	0.94	60.17
30		H	Br	H	H	H	0.21	0.73	45.05
31		H	OCH <sub>3</sub>	H	H	H	N.D.	N.D.	34.50
32		H	Br	H	H	H	1.00	0.99	33.68
33		H	Br	H	H	H	0.21	0.60	25.97

34		Br	H	H	H	H	N.D.	0.85	63.69
35		H	OH	H	H	H	N.D.	1.05	1.75
36		H	OCOCH <sub>3</sub>	H	H	H	N.D.	1.02	9.20

(a) Luciferase activity in everolimus-treated and control group was respectively 1 (normalized) and 0.40. Compounds were tested at 10  $\mu$ M concentration.

(b) Cyto-ID quantified autophagy in everolimus-treated and control group was respectively 1 (normalized) and 0.37. Compounds were tested at 10  $\mu$ M concentration.

(c) 3-MA: 3-Methyladenine (assay concentration 10 mM)

(d) N.D.: value was not determined

(e) UAMC-2526 was reported earlier by us in [13] and is used here as a reference.

When inspecting the data in **Table 1**, it should be noted first that results obtained in cellular assays must be interpreted with caution. First of all, compound performance is strongly dependent on a molecule's cellular permeability and/or tendency for intracellular accumulation. In addition, the data have been obtained from cells treated with everolimus. The latter stimulates autophagy in a largely homogenous manner throughout the full population. While this approach is generally recognized to be the most adequate one for reproducibly and reliably evaluating autophagy inhibitors, obtained results do not necessarily correlate with hypothetical compound potencies in normal, unstimulated cells. Autophagic flux in these normal cell populations and autophagosome pool turnover rates can be expected to be significantly different. Nonetheless, it can reasonably be anticipated that the inhibitory response to the compounds in non-everolimus primed cells will be relatively more potent. This has for example been illustrated by *ex vivo* histology on liver tissue from UAMC-2526-treated animals [13]

A general observation when looking at overall autophagy blocking potential (determined in the Cyto-ID assay), is that the most potent benzotropolones (e.g., **12-14**) at 10  $\mu$ M inhibit autophagy at least as effectively as 3-methyladenine (3-MA), used at 10 mM. 3-MA is a reference autophagy blocker used as a positive control in the experiment. The latter compound does not act through Atg4B-inhibition, but targets type III phosphatidylinositol 3-kinases (PI-3K). Of note, the Cyto-ID scores and Luciferase-reporter assay scores tend to correlate well within the ester series (**6-20**), but are not in agreement for some representatives of the amide series (**21-34**). This can be illustrated by comparing both parameters for **23-25**, **27** or **29**. A possible explanation could be that only Atg4B endopeptidase activity is measured in the luciferase reporter assay. However, as Atg4B is also involved in autophagy through LC3B-II deconjugase activity, the latter feature could account for different scores in both assay types in some cases. Although this is only a tentative rationale for the discrepancy, the more efficient autophagy blocking potential of the esters in our opinion seems to favour the latter compounds over their amide counterparts. Compound **32** (the amide analogue of UAMC-2526) is a relevant example of this observation: compared to its ester parent compound, the amide loses most of its Atg4B- and autophagy blocking potency. A notable exception nonetheless is amide **26**, which is both a strong autophagy inhibitor and one of the most effective inhibitors of intracellular Atg4B-activity in **Table 1**. The ester

analogue of **26** was reported earlier by us in reference [13], but was not among the most promising molecules identified in that report. An additional study goal relating to the R<sub>1</sub>-chain was to determine whether the *O*- or *N*-substituents in the esters and/or amides can be optimized. When comparing data for compound subsets with different R<sub>1</sub>-chains (but otherwise identically decorated benzotropolone rings, *e.g.*, **10-12** and **21-24**), there is no clear indication that the *O*- or *N*- substituent chain plays a pivotal role in target binding: this is generally reflected by the SDS-PAGE data and cellular potency data. Therefore, this part of the compound could therefore be suited for finetuning lipophilicity during the lead optimization phase, without affecting potency. Regardless of the foregoing, the carboxyl function present in most R<sub>1</sub>-groups of the series does seem to be involved in target binding. If it is removed (as in compounds **35** and **36**), most of the Atg4B and autophagy blocking potential is abolished.

Investigating the effect of functionalisation at the R<sub>2</sub>-position (as in **15-18** and **34**) was another goal of the study. The introduction of a Br-, Cl-, methoxy or *tert*-butyl substituent at R<sub>2</sub> is tolerated, but nonetheless generally decreases compound performance on all three parameters investigated. This can be illustrated by comparing the results for **6** (R<sub>2</sub>= -H) and **16** (R<sub>2</sub>= -Cl). The opposite trend however seems to be present for the introduction of a halogen atom at the R<sub>3</sub>-position. When comparing the corresponding pairs **21/28**, **23/29** and **24/30**, the halogenated compounds overall have better scores than analogues with R<sub>3</sub>=H. Lastly, the series included three derivatives with acetylated -OH groups at R<sub>4</sub>-R<sub>6</sub> or R<sub>3</sub> (**19-20** and **36**, respectively) that were prepared as potential prodrugs with increased cellular permeability. Intracellular hydrolysis would then be required to release the active molecule. None of these compounds however displayed notable activity. Compounds **19** and **20** are the direct analogues of two molecules that we reported in reference [13] (as UAMC-1356 and UAMC-1409, respectively) and were found to have a satisfactory autophagy inhibiting profile. The lack of activity for **19** and **20** therefore seems to imply that the hypothesized intracellular hydrolysis of the acetate prodrugs is not taking place at appreciable rates.

### 3. Conclusion

In this study, we report 29 novel autophagy inhibitors with a benzotropolone-based structure. The benzotropolone core of the molecules was installed relying on a one-pot oxidative condensation of a gallate and a catechol-derived precursor. For all prepared molecules, activity was determined on three complementary levels: intracellular Atg4B-inhibition, autophagy inhibitory potency and *in vitro* inhibition of Atg4B. At 10 μM concentration, the best compounds in the series block autophagy with comparable potency as reference 3-MA used at 10 mM. Within the set of novel molecules, compounds bearing an ester function at R<sub>1</sub> generally performed better than their amide counterparts. A notable exception is amide **26**, which outperforms reference UAMC-2526 in all three assay types and is among

the most promising compounds identified in this study. In addition, this work also indicates that the *O*- or *N*-substituent at R<sub>1</sub> is not critically involved in target binding. Therefore, this position can offer an opportunity for lipophilicity tuning of inhibitors, which is a potentially interesting feature for compounds with an obligatory intracellular mode-of-action. Finally, this manuscript shows that for introduction of a lipophilic substituent, the R<sub>3</sub>-position is generally more favoured than the R<sub>2</sub> position. Acetylation of the OH-groups at R<sub>4</sub>-R<sub>6</sub> is another modification type that can be used to increase lipophilicity and/or cellular permeability. The potential prodrugs that are obtained in this way, however, do not show activity. The latter indicates that either their cellular permeability is unexpectedly low or that they are not efficiently hydrolysed into the active benzotropolone inside the cells.

### Acknowledgments

We are grateful to the EU H2020-MSCA-IF actions (project ONCOPHAGY) and the Fund for Scientific Research Vlaanderen (FWO Vlaanderen) for supporting this work with a research grant. The Hercules Foundation is acknowledged for heavy equipment grants (NMR, preparatory purification infrastructure).

### References

- [1] N. Mizushima, M. Komatsu; Autophagy: renovation of cells and tissues. *Cell* 147, (2011) 728–741.
- [2] F. Randow, R.J. Youle; Self and nonself: how autophagy targets mitochondria and bacteria. *Cell Host Microbe* 15, (2014) 403–411.
- [3] Y. Ohsumi; Historical landmarks of autophagy research, *Cell Res.* 24, (2014) 9–23.
- [4] W. Martinet, P. Agostinis, B. Vanhooche, M. Dewaele, G.R.Y. De Meyer, Autophagy in disease: a double-edged sword with therapeutic potential, *Clin. Sci.* 116 (2009) 697-712.
- [5] X. Sui, R. Chen, Z. Wang, Z. Huang, N. Kong, M. Zhang, et al., Autophagy and chemotherapy resistance: a promising therapeutic target for cancer treatment, *Cell Death Dis.* 4 (2013), 838.
- [6] G. Manic, F. Obrist, G. Kroemer, I. Vitale, L. Galluzzi; Chloroquine and hydroxychloroquine for cancer therapy, *Mol. Cell Oncol.* 1 (2014), 29911. Taylor & Francis.
- [7] P. Pellegrini, A. Strambi, C. Zipoli, M. Hägg-Olofsson, M. Buoncervello, S. Linder, A. De Mito; Acidic extracellular pH neutralizes the autophagy-inhibiting activity of chloroquine, *Autophagy* 10 (2014), 562-571.
- [8] K. Satoo, N. N. Noda, H. Kumeta, Y. Fujioka, N. Mizushima, Y. Ohsumi, F. Inagaki, The structure of Atg4B–LC3 complex reveals the mechanism of LC3 processing and delipidation during autophagy, *EMBO J.* 28 (2009) 1341.

- [9] T. Maruyama, N. N. Noda, Autophagy-regulating protease Atg4: structure, function, regulation and inhibition, *J. Antibiot.* 71 (2018), 72–78.
- [10] D. Bosc, L. Vezenkov, S. Bortnik, J. An, J. Xu, C. Choutka, A. M. Hannigan, S. Kovacic, S. Loo, P. G. K. Clark, G. Chen, R. N. Guay-Ross, K. Yang, W. H. Dragowska, F. Zhang, N. E. Go, A. Leung, N. S. Honson, T. A. Pfeifer, M. Gleave, M. Bally, S. J. Jones, S. M. Gorski, R. N. Young; A new quinoline-based chemical probe inhibits the autophagy-related cysteine protease ATG4B, *Sci. Rep.* 8 (2018), 11653
- [11] J. Chu, Y. Fu, J. Xu, X. Zheng, Q. Gu, X. Luo, Q. Dai, S. Zhang, P. Liu, L. Hong, M. Li; ATG4B inhibitor FMK-9a induces autophagy independent on its enzyme inhibition, *Arch. Biochem. Biophys.* 644 (2018), 29-36.
- [12] M. Cleenewerck, M.O.J. Grootaert, R. Gladysz, Y. Adriaenssens, R. Roelandt, J. Joossens, A.M. Lambeir, G. R.Y. De Meyer, W. Declercq, K. Augustyns, W. Martinet, P. V. Der Veken; Inhibitor screening and enzymatic activity determination for autophagy target Atg4B using a gel electrophoresis-based assay, *Eur. J. Med.* 123 (2016) 631–638.
- [13] A. Kurdi, M. Cleenewerck, C. Vangestel, S. Lyssens, W. Declercq, J.P. Timmermans, S. Stroobants, K. Augustyns, G. R.Y. De Meyer, P. V. Der Veken, W. Martinet; ATG4B inhibitors with a benzotropolone core structure block autophagy and augment efficiency of chemotherapy in mice *Biochem. Pharmacol.* 138 (2017), 150-162.
- [14] Z. Qiu, B. Kuhn, J. Aebi, X. Lin, H. Ding, Z. Zhou, Z. Xu, D. Xu, L. Han, C. Liu, H. Qiu, Y. Zhang, W. Haap, C. Riemer, M. Stahl, N. Qin, H.C. Shen, G. Tang; Discovery of Fluoromethylketone-Based Peptidomimetics as Covalent ATG4B (Autophagin-1) Inhibitors. *ACS Med Chem Lett.* 8 (2016), 802-806
- [15] T. G. Nguyen, N. S. Honson, S. Arns, T. L. Davis, S. Dhe-Paganon, S. Kovacic, N. S. Kumar, T. A. Pfeifer, R. N. Young ; Development of Fluorescent Substrates and Assays for the Key Autophagy-Related Cysteine Protease Enzyme, ATG4B *Assay Drug Dev. Techn.* 12 (2014), 176-189
- [16] R. Ketteler, B. Seed, Quantitation of autophagy by luciferase release assay. *Autophagy*, 4 (2008), 801-806.

# Supporting Information for

## **Synthesis and screening of novel benzotropolones as Atg4B inhibitors to diminish autophagy process**

Muhammet Tanc,<sup>a†</sup> Matthias Cleenewerck,<sup>a†</sup> Ammar Kurdi,<sup>b</sup> Ria Roelandt,<sup>c, d</sup> Wim Declercq,<sup>c, d</sup> Guido De Meyer,<sup>b</sup> Koen Augustyns,<sup>a</sup> Wim Martinet,<sup>b\*</sup> Pieter van der Veken.<sup>a\*</sup>

<sup>a</sup> Laboratory of Medicinal Chemistry (UAMC), Department of Pharmaceutical Sciences, University of Antwerp, Antwerp, Belgium

<sup>b</sup>Laboratory of Physiopharmacology, Department of Pharmaceutical Sciences, University of Antwerp, Antwerp, Belgium

<sup>c</sup>VIB Inflammation Research Center, Technologiepark 927, B-9052, Ghent, Belgium

<sup>d</sup>Department of Biomedical Molecular Biology, Ghent University, Technologiepark 927, B-9052, Ghent, Belgium

## Table of Contents

1	Experimental data.....	2
	1.1 Chemistry.....	2
	1.2. Biochemistry.....	23
	1.2.1 Screening protocols.....	23
	1.2.1.1 SDS-PAGE-based screening assay for Atg4B inhibition.....	23
	1.2.1.2 CYTO-ID-based phenotypical screening for autophagy inhibition.....	24
	1.2.1.3 Luciferase reporter assay for assessment of intracellular Atg4B inhibition....	24

## 1. Experimental

### 1.1. Chemistry

All reagents and Anhydrous solvents were purchased from Acros Chemicals, Sigma–Aldrich, Fluorochem and TCI chemicals. All reactions involving air- or moisture- sensitive compounds were performed under a nitrogen atmosphere using dried glassware and syringes. Synthesized compounds were characterized with <sup>1</sup>H-NMR, <sup>13</sup>C-NMR and mass spectrometry. NMR spectra (<sup>1</sup>H NMR, <sup>13</sup>C NMR, DEPT-135, DEPT-90, HSQC, HMBC) were recorded on a 400 MHz Bruker Avance DRX-400 spectrometer. Chemical shifts are expressed in parts per million (ppm) and coupling constants (J) are in Hertz (Hz). Splitting patterns are mentioned as follows: s, singlet; d, doublet; sept, septet; t, triplet; q, quadruplet; m, multiplet; br s, broad singlet; dd, double of doublet, appt, aparent triplet, appq, aparent quartet, br t broad triplet. ES mass spectra were obtained from an Esquire 3000plus iontrap mass spectrometer from Bruker Daltonics. Purity was determined using two diverse HPLC systems using, respectively, a mass and UV-detector. Water (A) and CH<sub>3</sub>CN (B) were used as eluents. LC-MS spectra were recorded on an Agilent 1100 Series HPLC system using a Alltech Prevail C18 column (2.1 × 50 mm, 3 μm) coupled with an Esquire 3000plus as MS detector and a 5-100 % B, 20 min gradient was used with a flow rate from 0.2 mL/min. Formic acid 0.1 % was added to solvents A and B. Waters acquity UPLC system coupled to a waters TQD ESI mass spectrometer and waters TUV detector was used. A waters acquity UPLC BEH C18 1.7 μm 2.1 x 50 mm column was used. Solvent A: water with 0.1% formic acid, solvent B: acetonitrile with 0.1 % formic acid. Method I: 0.15 min 95 % A, 5 % B then in 1.85 min from 95 % A, 5 % B to 95 % B, 5 % A, then 0.25 min (0.350 mL/min), 95 % B, 5 % A. The wavelength for UV detection was 254 nm. Method II: flow 0.4 mL/min, 0.25 min 95 % A, 5 % B, then in 4.75 min to 95 % B, 5 % A, then 0.25 min 95 % B, 5 % A, followed by 0.75 min 95% A, 5 % B. The wavelength for UV detection was 214 nm. Where necessary flash purification was performed on a Biotage® ISOLERA One flash system equipped with internal variable dual-wavelength diode array detector (200-400 nm). SNAP cartridges (4-50 g) were used. Gradients used varied by purification.



## General procedure for the synthesis of compounds

### General procedure A: gallic acid esterification

In 50 mL of the alcohol of interest, 3,4,5-Trihydroxybenzoic acid **1** (1.5 g, 8.85 mmol) was dissolved, followed by addition of 10 drops of sulfuric acid. The solution was refluxed overnight. Afterwards, the solution was allowed to cool to room temperature. The residual alcohol was evaporated, yielding the gallic acid ester derivatives **1a-1c** as a solid compound.

### General procedure B: gallamide synthesis

To a stirred solution of the amine of interest (1.5 eq.) in 20 mL of dry DCM was added 1 eq. of 5-(Chlorocarbonyl)benzene-1,2,3-triyl triacetate **3** followed by addition of 1.5 eq. of *N*-Ethyl-*N*-isopropylpropan-2-amine. The solution was stirred for 1 h at room temperature and was afterwards evaporated to dryness to give an oily mixture. Then reaction mixture was extracted using 3 x 20 mL DCM and subsequently 20 mL 1M HCl, 20 mL saturated NaCl and Na<sub>2</sub>SO<sub>4</sub>. The organic layers were pooled and evaporated to dryness to yield the desired intermediate **4a-4g** as a yellow oil.

The obtained intermediate **4a-4g** was dissolved in 20 mL of acetonitrile while stirring at room temperature. Afterwards, 6 eq. of hydrazine monohydrate were added to the reaction mixture. After allowing the mixture to stir for 30 minutes at room temperature, 2 M HCl was added until a pH value of 3 was obtained. The mixture was extracted with 3 x 20 mL of ethyl acetate, and the combined organic layers were washed with 10 mL of saturated NaCl solution, followed by drying over MgSO<sub>4</sub>. Volatiles were evaporated using a rotary evaporator to give the desired deacetylated gallamide **5a-5g** [1,2]

### General procedure C: benzotropolone condensation **6, 7, 22-34**

Intermediate **1a-1c, 5a-5g** (1 eq.) and related catechol derivative (1 eq.) were dissolved in a mixture of 5 mL acetone and 20 mL water. A solution of potassium iodate (1 eq.) in 20 mL water was added dropwise to the reaction mixture over the course of 1 hour while stirring at room temperature. The mixture was stirred for an extra 1.5 h after addition of the potassium iodate and was then left standing for 30 minutes, allowing the target compound to precipitate. The reaction mixture was filtered and the precipitate was washed 3 times with 1 M HCl. After drying under high vacuum, the

desired benzotropolone **8**, **9**, **24-37** was obtained. If necessary, further purification steps were executed.

#### **Ethyl 3,4,5-trihydroxybenzoate (1a)**

Following **general procedure A**, ethanol was used for synthesis of the desired Ethyl 3,4,5-trihydroxybenzoate (0.600 g, 3.02 mmol), which was obtained as a white solid. (Yield: 34.1 %)

**<sup>1</sup>H NMR (400 MHz, DMSO-*d*<sub>6</sub>)** δ 1.26 (t, *J* = 7.1 Hz, 3H), 4.20 (q, *J* = 7.1 Hz, 2H), 6.94 (s, 2H), 9.16 (s, 3H). *t*<sub>R</sub> 0.86 min, UPLC (ESI) *m/z* 395.5 [2M-H]<sup>-</sup> (100 %)

#### **Propyl 3,4,5-trihydroxybenzoate (1b)**

Following **general procedure A**, Propan-1-ol was used for synthesis of Propyl 3,4,5-trihydroxybenzoate (1.416 g, 6.67 mmol). (Yield: 75 %)

**<sup>1</sup>H NMR (400 MHz, DMSO-*d*<sub>6</sub>)** δ 0.93 (t, *J* = 7.4 Hz, 3H), 1.65 (sx, *J* = 7.3 Hz, 2H), 4.10 (t, *J* = 6.5 Hz, 2H), 6.95 (s, 2H), 7.44 (d, *J* = 28.2 Hz, 3H). *t*<sub>R</sub> 1.29 min, UPLC (ESI) *m/z* 213.1 [M+H]<sup>+</sup> (95 %)

#### **Butyl 3,4,5-trihydroxybenzoate (1c)**

Following **general procedure A**, Butan-1-ol was used for synthesis of Butyl 3,4,5-trihydroxybenzoate (1.846 g, 8.16 mmol). (Yield: 92 %)

**<sup>1</sup>H NMR (400 MHz, DMSO-*d*<sub>6</sub>)** δ 0.92 (t, *J* = 7.4 Hz, 3H), 1.38 (sx, *J* = 7.2 Hz, 2H), 1.64 (dt, *J* = 6.5, *J*' = 6.5 Hz, 2H), 4.16 (t, *J* = 6.5 Hz, 2H), 6.94 (s, 2H), 8.94 (s, 1H), 9.26 (s, 2H). *t*<sub>R</sub> 1.14 min, UPLC (ESI) *m/z* 227.3 [M+H]<sup>+</sup> (96 %)

#### **3,4,5-Triacetoxybenzoic acid (2)**

One equivalent of 3,4,5-Trihydroxybenzoic acid **2** (6 g, 35.3 mmol) was suspended in 7.5 equivalents of acetic anhydride. The obtained suspension was stirred and 10 drops of sulphuric acid were added catalytically. The solution was heated at 80°C for 15 minutes, then left to cool to room temperature. 150 mL of ice water was added to the solution, initiating the formation of a white precipitate. The mixture was left standing for 2 hours, allowing formation of white crystals. The precipitate was filtered off and dried under high vacuum to yield 3,4,5-Triacetoxybenzoic acid (8.38 g, 28.26 mmol) as white crystals. (Yield: 80 %)

**<sup>1</sup>H NMR (400 MHz, DMSO-*d*<sub>6</sub>)** δ 2.30 (s, 6H), 2.33 (s, 3H), 7.75 (s, 2H), 13.40 (s, 1H). *t*<sub>R</sub> 1.45 min, UPLC (ESI) *m/z* 295.0 [M-H]<sup>-</sup> (100 %)

### 5-(Chlorocarbonyl)benzene-1,2,3-triyl triacetate (3)

3,4,5-triacetoxybenzoic acid **2** (8.38 g, 28.26 mmol) was suspended in 30 mL of dry toluene. Afterwards, 3 equivalents of thionyl chloride were added dropwise. The mixture was refluxed for 90 minutes, then allowed to cool to room temperature. Volatiles were evaporated using a rotary evaporator, with formation of a white precipitate to give 5-(Chlorocarbonyl)benzene-1,2,3-triyl triacetate (7.83 g, 24.89 mmol) as a white precipitate and directly used for further steps. (Yield: 88 %)

### 3,4,5-Trihydroxybenzamide (5a).

Following **general procedure B**, ammonia (61.0 mL, 30.5 mmol) was used to afford the intermediate 5-Carbamoylbenzene-1,2,3-triyl triacetate **4a** (5.6 g, 18.97 mmol, yield: 93 %), which was deacetylated to obtain the desired 3,4,5-Trihydroxybenzamide (0.500 g, 2.96 mmol) as a pure solid. (Yield: 16 %)

**<sup>1</sup>H NMR (400 MHz, DMSO-*d*<sub>6</sub>)** δ 6.55 (s, 2H), 8.44 (s, 2H), 8.71 (s, 1H), 9.40 (s, 2H). *t*<sub>R</sub> 0.25 min, UPLC (ESI) *m/z* 168.1 [M-H] (100 %)

### 3,4,5-Trihydroxy-*N*-methylbenzamide (5b).

Following **general procedure B**, methylamine (2.59 mL, 5.17 mmol) was used to afford the intermediate 5-(Methylcarbamoyl)benzene-1,2,3-triyl triacetate **4b** (1.066 g, 3.45 mmol, yield: 100 %), which was deacetylated to obtain the desired 3,4,5-Trihydroxy-*N*-methylbenzamide (0.46 g, 2.51 mmol) as a yellow, viscous oil. (Yield: 73 %)

**<sup>1</sup>H NMR (400 MHz, DMSO-*d*<sub>6</sub>)** δ 2.68 (d, *J* = 4.5 Hz, 3H), 6.79 (s, 2H), 8.02 (t, *J* = 4.5 Hz, 1H), 8.78 (s, 1H), 9.03 (s, 2H). *t*<sub>R</sub> 0.26 min, UPLC (ESI) *m/z* 182.2 [M-H]<sup>-</sup> (100 %)

### *N*-Ethyl-3,4,5-trihydroxybenzamide (5c)

Following **general procedure B**, ethylamine (2M in THF, 2.86 mL, 5.72 mmol) was used to afford the intermediate 5-(Ethylcarbamoyl)benzene-1,2,3-triyl triacetate **4c** (1.233 g, 3.81 mmol, yield: 100 %), which was deacetylated to obtain the desired *N*-Ethyl-3,4,5-trihydroxybenzamide (0.420 g, 2.13 mmol) as a yellow oil. (Yield: 55.8 %)

**<sup>1</sup>H NMR (400 MHz, DMSO-*d*<sub>6</sub>)** δ 1.06 (t, *J* = 7.2 Hz, 3H), 3.09 – 3.24 (m, 2H), 6.80 (s, 2H), 7.87 (s, 1H), 8.06 (t, *J* = 5.1 Hz, 1H). *t*<sub>R</sub> 0.26 min, UPLC (ESI) *m/z* 198.1 [M+H]<sup>+</sup> (96 %)

### ***N*-Propyl-3,4,5-trihydroxybenzamide (5d)**

Following **general procedure B**, *N*-Propyl amine (0.470 mL, 5.72 mmol) was used to afford the intermediate 5-(Propylcarbamoyl)benzene-1,2,3-triyl triacetate **4d** (1.286 g, 3.81 mmol, yield: 100 %), which was deacetylated to obtain the desired 5-(Propylcarbamoyl)benzene-1,2,3-triyl triacetate (0.491 g, 2.32 mmol) as a colourless oil. (Yield: 61 %)

**<sup>1</sup>H NMR (400 MHz, DMSO-*d*<sub>6</sub>)** δ 0.83 (t, *J* = 7.4 Hz, 3H), 1.57 (sx, *J* = 7.4 Hz, 2H), 3.44 (q, *J* = 6.5 Hz, 2H), 6.82 (s, 2H), 7.82 (s, 1H), 8.06 (s, 1H), 9.01 (s, 2H). *t*<sub>R</sub> 0.75 min, UPLC (ESI) *m/z* 212.1 [M+H]<sup>+</sup> (95 %)

### ***N*-Butyl-3,4,5-trihydroxybenzamide (5e)**

Following **general procedure B**, Butan-1-amine (0.507 g, 6.93 mmol) was used to afford the intermediate 5-(Butylcarbamoyl)benzene-1,2,3-triyl triacetate **4e** (1.91 g, 5.46 mmol, yield: 78 %), which was deacetylated to obtain the desired *N*-Butyl-3,4,5-trihydroxybenzamide (1.10 g, 4.92 mmol). (Yield: 90 %)

**<sup>1</sup>H NMR** Data in agreement with reference [3], UPLC (ESI) *m/z* 224.2 [M-H]<sup>-</sup> (100 %)

### **3,4,5-Trihydroxy-*N*-isobutylbenzamide (5f).**

Following **general procedure B**, isobutylamine (0.293 g, 4.01mmol) was used to afford the intermediate 5-(Isobutylcarbamoyl)benzene-1,2,3-triyl triacetate **4f** (0.638 g, 1.816 mmol, yield: 68 %), which was deacetylated to obtain the desired 3,4,5-Trihydroxy-*N*-isobutylbenzamide (0.278 g, 1.23 mmol) as a pure solid. (Yield: 68 %)

**<sup>1</sup>H NMR (400 MHz, DMSO-*d*<sub>6</sub>)** δ 0.85 (d, *J* = 6.7 Hz, 6H), 1.79 (m, 1H), 2.99 (t, *J* = 6.8 Hz, 2H), 6.81 (s, 2H), 7.80 (s, 1H), 8.03 (t, *J* = 5.8 Hz, 1H), 8.90 (s, 2H). *t*<sub>R</sub> 1.22 min, UPLC (ESI) *m/z* 226.1 [M+H]<sup>+</sup> (100 %)

### ***N*-Hexyl-3,4,5-trihydroxybenzamide (5g)**

Following **general procedure B**, Hexan-1-amine (0.670 g, 6.62 mmol) was used to afford the intermediate 5-(Hexylcarbamoyl)benzene-1,2,3-triyl triacetate **4g** (1.88 g, 4.96 mmol, yield: 75 %), which was deacetylated to obtain the desired *N*-Hexyl-3,4,5-trihydroxybenzamide (1.23 g, 4.86 mmol) as a solid powder. (Yield: 98 %)

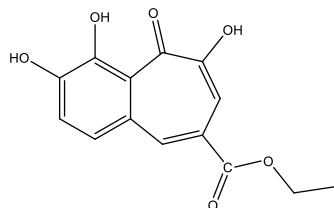
**<sup>1</sup>H NMR (400 MHz, DMSO-*d*<sub>6</sub>)** δ 0.85 (t, *J* = 7.5 Hz, 3H), 1.18 – 1.29 (m, 4H), 1.34 (m, 2H), 1.49 – 1.40 (m, 2H), 3.15 (dd, *J* = 13.0, *J'* = 6.8 Hz, 2H), 6.80 (s, 2H), 7.76 (d, *J* = 46.1 Hz, 2H), 8.03 (t, *J* = 5.6 Hz, 1H), 9.00 (s, 1H). *t*<sub>R</sub> 1.38 min, UPLC (ESI) *m/z* 254.2 [M+H]<sup>+</sup> (93 %)

#### ***N*-Benzyl-3,4,5-trihydroxybenzamide (5h).**

Following **general procedure B**, benzylamine (0.358 g, 3.34 mmol) was used to afford the intermediate 5-(Benzylcarbamoyl)benzene-1,2,3-triyl triacetate **4h** (0.857 g, 2.225 mmol, yield: 100 %), which was deacetylated to obtain the desired *N*-Benzyl-3,4,5-trihydroxybenzamide (0.525 g, 2.024 mmol) white solid. (Yield: 91 %)

**<sup>1</sup>H NMR (400 MHz, DMSO-*d*<sub>6</sub>)** δ 4.39 (d, *J* = 6.0 Hz, 2H) 6.86 (s, 2H), 7.18 - 7.33 (m, 5H), 8.62 (t, *J* = 6.0 Hz, 1H), 8.97 (s, 2H). *t*<sub>R</sub> 1.28 min, UPLC (ESI) *m/z* 260.0 [M+H]<sup>+</sup> (100 %)

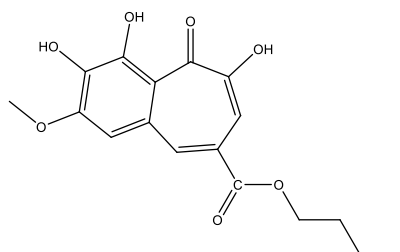
#### **Ethyl 3,4,6-trihydroxy-5-oxo-5*H*-benzo[7]annulene-8-carboxylate (6)**



Following **general procedure C**, Ethyl 3,4,5-trihydroxybenzoate **1a** (0.464g, 2.341 mmol) and pyrocatechol (0.258 g, 2.341 mmol) were used. The crude solid was purified by flash chromatography on silica gel using EtOAc/heptane (1:4) as eluent. The pure fractions were pooled and concentrated to give the desired ethyl 3,4,6-Trihydroxy-5-oxo-5*H*-benzo[7]annulene-8-carboxylate (0.188 g, 0.681 mmol) as an amorphous powder. (Yield: 29 %)

**<sup>1</sup>H NMR (400 MHz, DMSO-*d*<sub>6</sub>)** δ 1.35 (t, *J* = 7.1 Hz, 3H), 4.34 (q, *J* = 7.1 Hz, 2H), 7.48 (dd, *J* = 8.6, *J'* = 2.8 Hz, 1H), 7.64 (ddd, *J* = 10.1, *J'* = 3.1, *J''* = 1.6 Hz, 2H), 8.28 – 8.33 (m, 1H), 9.73 (d, *J* = 30.4 Hz, 1H), 10.42 (d, *J* = 25.8 Hz, 1H), 14.80 (d, *J* = 16.8 Hz, 1H). **<sup>13</sup>C NMR (101 MHz, DMSO-*d*<sub>6</sub>)** δ 14.1, 61.7, 115.3, 115.9, 120.3, 121.9, 128.5, 138.7, 148.7, 151.2, 153.2, 165.9, 167.6, 184.9. *t*<sub>R</sub> 1.78 min, UPLC (ESI) *m/z* 275.5 [M-H]<sup>-</sup> (100 %)

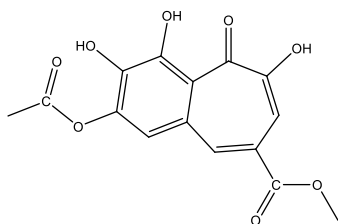
### Butyl 3,4,6-trihydroxy-2-methoxy-5-oxo-5H-benzo[7]annulene-8-carboxylate (7)



Following **general procedure C**, Butyl 3,4,5-trihydroxybenzoate **1c** (0.484 g, 2.141 mmol) and 3-methoxybenzene-1,2-diol (0.3 g, 2.141 mmol) were used. The desired butyl 3,4,6-Trihydroxy-2-methoxy-5-oxo-5H-benzo[7]annulene-8-carboxylate (0.446 g, 1.334 mmol) was obtained as an amorphous powder. (Yield: 62 %)

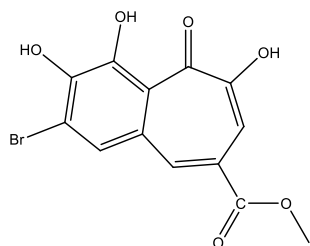
**<sup>1</sup>H NMR (400 MHz, DMSO-*d*<sub>6</sub>)** δ 0.95 (t, *J* = 7.4 Hz, 3H), 1.40 – 1.48 (m, 2H), 1.74 (m, 2H), 4.01 (s, 3H), 4.31 (t, *J* = 6.7 Hz, 2H), 7.44 (s, 1H), 7.58 (s, 1H), 8.36 (s, 1H). **<sup>13</sup>C NMR (101 MHz, DMSO-*d*<sub>6</sub>)** δ 13.6, 18.7, 30.2, 56.2, 65.4, 109.9, 113.9, 116.1, 123.6, 129.7, 137.7, 137.9, 151.4, 151.9, 153.6, 166.1, 183.0. *t*<sub>R</sub> 2.21 min, UPLC (ESI) *m/z* 333.5 [M-H]<sup>-</sup> (100 %)

### Methyl 2-acetoxy-3,4,6-trihydroxy-5-oxo-5H-benzo[7]annulene-8-carboxylate (9)



Following **general procedure C**, Methyl 3,4,5-trihydroxybenzoate (0.527 g, 2.86 mmol) and 2,3-dihydroxyphenyl acetate (0.481 g, 2.86 mmol) were used. The desired Methyl 2-acetoxy-3,4,6-trihydroxy-5-oxo-5H-benzo[7]annulene-8-carboxylate (0.549 g, 1.714 mmol) was obtained as an amorphous powder. (Yield: 60 %) **<sup>1</sup>H NMR (400 MHz, DMSO-*d*<sub>6</sub>)** δ 2.34 (s, 3H), 3.90 (s, 3H), 7.10 (s, 1H), 7.46 (s, 1H), 8.12 (s, 1H), 10.00 (s, 1H), 11.48 (s, 1H), 15.28 (s, 1H). **<sup>13</sup>C NMR (101 MHz, DMSO-*d*<sub>6</sub>)** δ 20.8, 51.7, 113.2, 121.3, 122.0, 122.8, 128.1, 128.5, 139.7, 148.3, 151.4, 153.7, 165.4, 169.1, 184.2. *t*<sub>R</sub> 1.65 min, UPLC (ESI) *m/z* 319.5 [M-H]<sup>+</sup> (100 %)

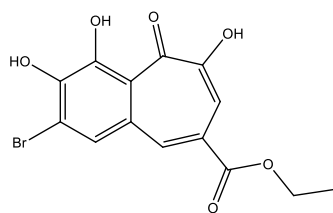
### Methyl 2-bromo-3,4,6-trihydroxy-5-oxo-5H-benzo[7]annulene-8-carboxylate (10)



Following **general procedure C**, Methyl 3,4,5-trihydroxybenzoate (0.300 g, 1.629 mmol) and 3-bromobenzene-1,2-diol (0.308 g, 1.629 mmol) were used. The desired Methyl 2-bromo-3,4,6-trihydroxy-5-oxo-5H-benzo[7]annulene-8-carboxylate (0.454 g, 1.331 mmol) was obtained as an amorphous powder. (Yield: 82 %)

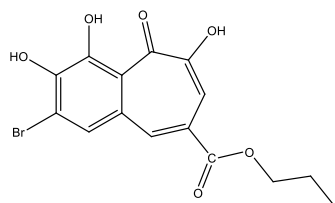
**<sup>1</sup>H NMR (400 MHz, DMSO-*d*<sub>6</sub>)** δ 3.88 (s, 3H), 7.63 (s, 1H), 8.08 (s, 1H), 8.30 (s, 1H), 9.95 (s, 1H), 10.97 (s, 1H), 15.27 (s, 1H). **<sup>13</sup>C NMR (101 MHz, DMSO-*d*<sub>6</sub>)** δ 53.0, 115.3, 116.7, 119.2, 123.8, 128.8, 130.1, 137.6, 145.7, 151.5, 153.8, 166.3, 184.7. *t*<sub>R</sub> 1.98 min, UPLC (ESI) *m/z* 340.8/342.8 (1:1) [M-H]<sup>-</sup> (93 %)

### Ethyl 2-bromo-3,4,6-trihydroxy-5-oxo-5H-benzo[7]annulene-8-carboxylate (11)



Following **general procedure C**, Ethyl 3,4,5-trihydroxybenzoate **1a** (0.210 g, 1.058 mmol) and 3-bromobenzene-1,2-diol (0.308 g, 1.629 mmol) were used. The desired Ethyl 2-bromo-3,4,6-trihydroxy-5-oxo-5H-benzo[7]annulene-8-carboxylate (0.256 g, 0.721 mmol) was obtained as an amorphous powder. (Yield: 68 %) **<sup>1</sup>H NMR (400 MHz, DMSO-*d*<sub>6</sub>)** δ 1.35 (t, *J* = 7.1 Hz, 3H), 4.33 (q, *J* = 7.1 Hz, 2H), 7.61 (s, 1H), 8.09 (s, 1H), 8.30 (s, 1H), 9.94 (s, 1H), 10.96 (s, 1H), 15.27 (s, 1H). **<sup>13</sup>C NMR (101 MHz, DMSO-*d*<sub>6</sub>)** δ 14.0, 61.8, 115.3, 116.7, 119.2, 124.1, 128.8, 130.0, 137.5, 145.7, 151.5, 153.8, 165.8, 184.7. *t*<sub>R</sub> 1.92 min, UPLC (ESI) *m/z* 355.0/357.0 (1:1) [M-H]<sup>-</sup> (91 %)

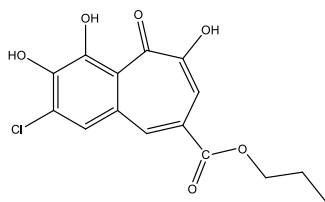
### Propyl 2-bromo-3,4,6-trihydroxy-5-oxo-5H-benzo[7]annulene-8-carboxylate (12)



Following **general procedure C**, Propyl 3,4,5-trihydroxybenzoate **1b** (0.168 g, 0.794 mmol) and 3-Bromobenzene-1,2-diol (0.150 g, 0.794 mmol) were used. The desired Propyl 2-bromo-3,4,6-trihydroxy-5-oxo-5H-benzo[7]annulene-8-carboxylate (0.198 g, 0.536 mmol) was obtained as an amorphous powder. (Yield: 68 %)

**<sup>1</sup>H NMR (400 MHz, DMSO-*d*<sub>6</sub>)** δ 0.99 (t, *J* = 7.4 Hz, 3H), 1.77 (sx, *J* = 7.3 Hz, 2H), 4.25 (t, *J* = 6.6 Hz, 2H), 7.62 (s, 1H), 8.10 (s, 1H), 8.29 (s, 1H), 9.95 (s, 1H), 10.96 (s, 1H), 15.27 (s, 1H). **<sup>13</sup>C NMR (101 MHz, DMSO-*d*<sub>6</sub>)** δ 10.4, 21.5, 67.2, 115.3, 116.7, 119.2, 124.0, 128.8, 130.1, 137.5, 145.7, 151.5, 153.8, 165.8, 184.7. *t*<sub>R</sub> 2.02 min, UPLC (ESI) *m/z* 369.0/371.0 (1:1) [M+H]<sup>+</sup> (90 %)

### Propyl 2-chloro-3,4,6-trihydroxy-5-oxo-5H-benzo[7]annulene-8-carboxylate (13)

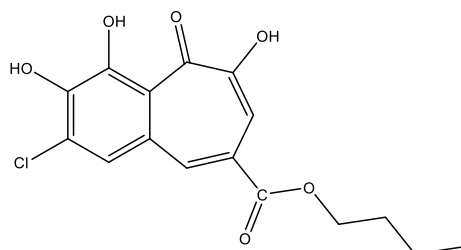


Following **general procedure C**, Propyl 3,4,5-trihydroxybenzoate **1b** (0.220 g, 1.038 mmol) and 3-Chlorobenzene-1,2-diol (0.150 g, 1.038 mmol) were used. The desired Propyl 2-chloro-3,4,6-trihydroxy-5-oxo-5H-benzo[7]annulene-8-carboxylate (0.221 g, 0.681 mmol) was obtained as an amorphous powder. (Yield: 66 %)

**<sup>1</sup>H NMR (400 MHz, DMSO-*d*<sub>6</sub>)** δ 0.99 (t, *J* = 7.4 Hz, 3H), 1.75 (sx, *J* = 7.4 Hz, 2H), 4.25 (t, *J* = 6.6 Hz, 2H), 7.61 (s, 1H), 7.96 (s, 1H), 8.30 (s, 1H), 9.96 (s, 1H), 10.93 (s, 1H), 15.25 (s, 1H). **<sup>13</sup>C NMR (101 MHz, DMSO-*d*<sub>6</sub>)** δ 10.3, 21.5, 67.2, 115.2, 118.9, 124.1, 126.4, 127.1, 128.5, 137.5, 144.5, 152.1, 153.8, 165.8, 184.5. *t*<sub>R</sub> 1.99 min, UPLC (ESI) *m/z* 325.0/327.0 (3:1) [M+H]<sup>+</sup> (100 %)



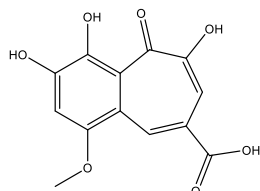
### Butyl 2-chloro-3,4,6-trihydroxy-5-oxo-5H-benzo[7]annulene-8-carboxylate (14)



Following **general procedure C**, Butyl 3,4,5-trihydroxybenzoate **1c** (0.313 g, 1.384 mmol) and 3-Chlorobenzene-1,2-diol (0.2 g, 1.384 mmol) were used. The desired Butyl 2-chloro-3,4,6-trihydroxy-5-oxo-5H-benzo[7]annulene-8-carboxylate (0.163 g, 0.481 mmol) was obtained as an amorphous powder. (Yield: 35 %).

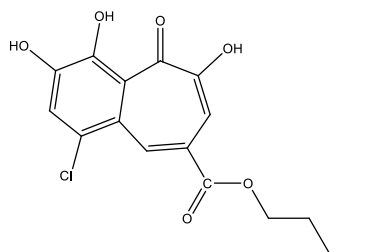
**<sup>1</sup>H NMR (400 MHz, DMSO-*d*<sub>6</sub>)**  $\delta$  0.95 (t, *J* = 7.4 Hz, 3H), 1.44 (sx, *J* = 7.4 Hz, 2H), 1.72 (p, *J* = 6.6 Hz, 2H), 4.30 (t, *J* = 6.6 Hz, 2H), 7.60 (s, 1H), 7.95 (s, 1H), 8.28 (s, 1H), 9.97 (s, 1H), 10.95 (s, 1H), 15.19 (s, 1H). **<sup>13</sup>C NMR (101 MHz, DMSO-*d*<sub>6</sub>)**  $\delta$  13.6, 18.7, 30.1, 65.5, 115.2, 118.9, 124.1, 126.4, 127.1, 128.5, 137.5, 144.5, 152.1, 153.8, 165.8, 184.6.  $t_R$  2.11 min, UPLC (ESI) *m/z* 339.1/341.1 (3:1) [M+H]<sup>+</sup>, (100 %)

### 3,4,6-Trihydroxy-1-methoxy-5-oxo-5H-benzo[7]annulene-8-carboxylic acid (15)



Following **general procedure C**, 3,4,5-Trihydroxybenzoic acid (0.4 g, 2.351 mmol) and 4-Methoxybenzene-1,2-diol (0.330 g, 2.351 mmol) were used. The crude precipitate was purified by flash chromatography on reversed phase C-18 silica gel using ACN/H<sub>2</sub>O (1:3) as eluent, followed by 100% MeOH + 0.1 % TEA to afford the desired 3,4,6-Trihydroxy-1-methoxy-5-oxo-5H-benzo[7]annulene-8-carboxylic acid (0.052 g, 0.187 mmol) as an amorphous powder. (Yield: 8 %) **<sup>1</sup>H NMR (400 MHz, DMSO-*d*<sub>6</sub>)**  $\delta$  3.95 (s, 3H), 7.27 (s, 1H), 7.67 (s, 1H), 9.00 (s, 1H), 9.58 (brs, 2H), 14.26 (brs, 1H). **<sup>13</sup>C NMR (101 MHz, DMSO-*d*<sub>6</sub>)**  $\delta$  57.0, 106.0, 116.5, 117.0, 120.2, 122.0, 129.7, 144.6, 150.1, 152.2, 152.5, 167.9, 185.0.  $t_R$  1.31 min, UPLC (ESI) *m/z* 277.3 [M-H]<sup>-</sup> (100 %)

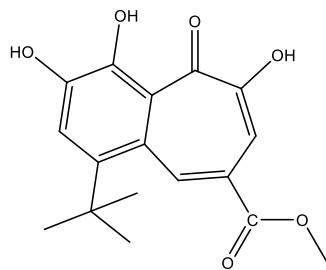
**Butyl 1-chloro-3,4,6-trihydroxy-5-oxo-5H-benzo[7]annulene-8-carboxylate (16)**



Following **general procedure C**, Butyl 3,4,5-trihydroxybenzoate **1c** (0.516 g, 2.283 mmol) and 4-Chlorobenzene-1,2-diol (0.33 g, 2.283 mmol) were used to afford the desired Butyl 1-chloro-3,4,6-trihydroxy-5-oxo-5H-benzo[7]annulene-8-carboxylate (0.111 g, 0.328 mmol) as an amorphous powder. (Yield: 14 %)

**<sup>1</sup>H NMR (400 MHz, DMSO-*d*<sub>6</sub>)** δ 0.95 (t, *J* = 7.42 Hz, 3H), 1.46 (m, 2H), 1.71 (m, 2H), 4.32 (m, 2H), 7.56 (s, 1H), 7.68 (s, 1H), 8.88 (s, 1H), 10.11 (s, 1H), 10.87 (s, 1H), 14.77 (s, 1H). **<sup>13</sup>C NMR (101 MHz, DMSO-*d*<sub>6</sub>)** δ 13.6, 18.7, 30.1, 65.5, 113.5, 121.5, 123.9, 126.3, 131.7, 137.4, 147.1, 150.3, 154.1, 164.7, 184.1. *t*<sub>R</sub> 2.18 min, UPLC (ESI) *m/z* 337.5/339.5 (3:1) [M-H]<sup>-</sup> (89 %)

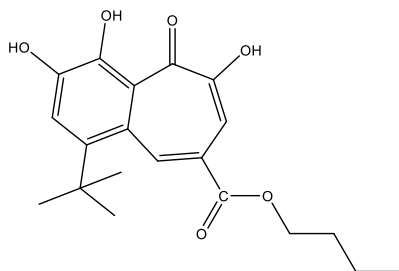
**Methyl 1-(tert-butyl)-3,4,6-trihydroxy-5-oxo-5H-benzo[7]annulene-8-carboxylate (17)**



Following **general procedure C**, Methyl 3,4,5-trihydroxybenzoate (0.222 g, 1.203 mmol) and 4-(*tert*-Butyl)benzene-1,2-diol (0.200 g, 1.203 mmol) were used. The obtained precipitate was purified by flash chromatography on silica gel using EtOAc/heptane (1:4) as eluent to yield the desired Methyl 1-(*tert*-butyl)-3,4,6-trihydroxy-5-oxo-5H-benzo[7]annulene-8-carboxylate (0.245 g, 0.770 mmol) as an amorphous powder after evaporation of the pooled pure fragments. (Yield: 64 %)

**<sup>1</sup>H NMR (400 MHz, DMSO-*d*<sub>6</sub>)** δ 1.55 (s, 9H), 3.90 (s, 3H), 7.52 (s, 1H), 7.63 (s, 1H), 9.08 (s, 1H). **<sup>13</sup>C NMR (101 MHz, DMSO-*d*<sub>6</sub>)** δ 32.4, 36.1, 53.0, 113.8, 119.8, 121.4, 123.3, 125.9, 134.5, 143.9, 147.6, 148.6, 153.4, 167.0, 186.1. *t*<sub>R</sub> 1.96 min, UPLC (ESI) *m/z* 319.1 [M+H]<sup>+</sup> (100 %)

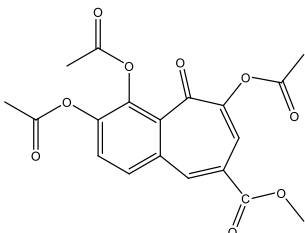
**Butyl 1-(*tert*-butyl)-3,4,6-trihydroxy-5-oxo-5*H*-benzo[7]annulene-8-carboxylate (18)**



Following **general procedure C**, Butyl 3,4,5-trihydroxybenzoate **1c** (0.272 g, 1.203 mmol) and 4-(*tert*-Butyl)benzene-1,2-diol (0.200 g, 1.203 mmol) were used. The obtained precipitate was purified by flash chromatography on silica gel using EtOAc/heptane (1:5) as eluent to afford the desired Butyl 1-(*tert*-butyl)-3,4,6-trihydroxy-5-oxo-5*H*-benzo[7]annulene-8-carboxylate (0.286 g, 0.794 mmol) as an amorphous powder after evaporation of the pooled pure fragments. (Yield: 66 %)

**<sup>1</sup>H NMR (400 MHz, DMSO-*d*<sub>6</sub>)** δ 0.94 (t, *J* = 7.4 Hz, 3H), 1.45 (sx, *J* = 7.3, 2H), 1.55 (s, 9H), 1.72 (p, *J* = 6.2, 2H), 4.29 (t, *J* = 6.4 Hz, 2H), 7.53 (s, 1H), 7.64 (s, 1H), 9.09 (s, 1H), 9.83 (s, 1H), 10.26 (s, 1H), 14.38 (s, 1H). **<sup>13</sup>C NMR (101 MHz, DMSO-*d*<sub>6</sub>)** δ 13.5, 18.7, 30.2, 32.3, 36.2, 65.4, 113.9, 120.0, 121.4, 123.3, 125.9, 134.2, 143.7, 147.6, 148.7, 153.4, 166.4 186.2. *t*<sub>R</sub> 2.27 min, UPLC (ESI) *m/z* 361.2 [M+H]<sup>+</sup> (100 %)

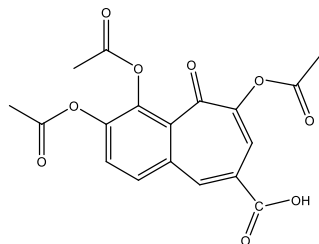
**8-(Methoxycarbonyl)-5-oxo-5*H*-benzo[7]annulene-3,4,6-triyl triacetate (19)**



To a stirred suspension of Methyl 3,4,6-trihydroxy-5-oxo-5*H*-benzo[7]annulene-8-carboxylate [2] (0.150 g, 0.57 mmol) in THF, 6 eq. of acetic anhydride and 6 eq. of DIPEA were added. The reaction mixture was stirred overnight at room temperature. Volatiles were evaporated and the reaction mixture was further purified by flash chromatography on silica gel using a EtOAc/hexane 1:1 solvent mixture. Pure fractions were pooled and evaporated using a rotary evaporator and after further drying under high vacuum, the desired 8-(Methoxycarbonyl)-5-oxo-5*H*-benzo[7]annulene-3,4,6-triyl triacetate (0.200 g, 0.515 mmol) was obtained as an amorphous powder [4]. (Yield: 90 %) **<sup>1</sup>H NMR (400 MHz, DMSO-*d*<sub>6</sub>)** δ 2.25 (s, 3H), 2.28 (s, 3H), 2.33 (s, 3H), 3.89 (s, 3H), 7.46 (s, 1H), 7.84 (d, *J* = 9.2 Hz, 1H), 8.12 (d, *J* = 9.2 Hz, 1H), 8.43 (s, 1H). **<sup>13</sup>C NMR (101 MHz, DMSO-*d*<sub>6</sub>)** δ 20.0, 21.1, 124.7,

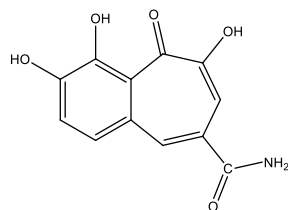
126.5, 129.8, 131.3, 140.1, 143.5, 146.1, 154.9, 168.1, 171.4, 179.6.  $t_R$  1.68 min, UPLC (ESI)  $m/z$  389.5 [M+H]<sup>+</sup> (100 %)

### 3,4,6-Triacetoxy-5-oxo-5H-benzo[7]annulene-8-carboxylic acid (20)



To a stirred suspension of 3,4,6-Trihydroxy-5-oxo-5H-benzo[7]annulene-8-carboxylic acid [2]. (0.150 g, 0.60 mmol) in THF, 6 eq. of acetic anhydride and 6 eq. of DIPEA were added. The reaction mixture was stirred overnight at room temperature. Volatiles were evaporated and the reaction mixture was further purified by flash chromatography on silica gel using a EtOAc/hexane 1:1 solvent mixture. Pure fractions were pooled and evaporated using a rotary evaporator and the desired 3,4,6-Triacetoxy-5-oxo-5H-benzo[7]annulene-8-carboxylic acid (0.212 g, 0.566 mmol) was obtained as an amorphous powder after further drying under high vacuum [4]. (Yield: 93 %) <sup>1</sup>H NMR (400 MHz, DMSO-*d*<sub>6</sub>) δ 2.24 (s, 3H), 2.26 (s, 3H), 2.32 (s, 3H), 7.75 (d, *J* = 8.7 Hz, 1H), 7.77 (d, *J* = 4.5 Hz, 1H), 7.97 (d, *J* = 8.9 Hz, 1H), 8.34 (s, 1H), 14.81 (s, 1H). <sup>13</sup>C NMR (101 MHz, DMSO-*d*<sub>6</sub>) δ 20.0, 20.1, 20.4, 53.1, 120.4, 124.3, 127.7, 130.9, 131.4, 132.5, 139.7, 141.1, 145.6, 147.7, 165.6, 167.8, 167.9, 168.0, 180.3.  $t_R$  1.49 min, UPLC (ESI)  $m/z$  373.3 [M-H]<sup>-</sup> (92 %)

### 3,4,6-Trihydroxy-5-oxo-5H-benzo[7]annulene-8-carboxamide (21)

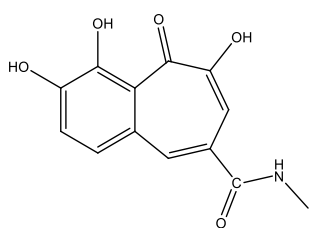


To a stirred solution of compound Methyl 3,4,6-trihydroxy-5-oxo-5H-benzo[7]annulene-8-carboxylate [2] (0.446 g, 1.701 mmol), 1.2 eq. of 7 N ammonia in MeOH were added. After 2 hours of refluxing the reaction mixture, formation of the target compound could be observed by HPLC analysis. Further progression of target compound formation was monitored by HPLC, and after 5 days, the reaction was terminated, with complete conversion of the starting compound. The mixture was evaporated to dryness using a rotary evaporator and the crude product was washed with hexane and water. The obtained product was suspended in water and extracted with 3 x 20 mL EtOAc. The

organic layers were combined and washed with 10 mL of saturated NaCl solution, followed by drying over MgSO<sub>4</sub>. The desired 3,4,6-Trihydroxy-5-oxo-5H-benzo[7]annulene-8-carboxamide (0.004 g, 0.016 mmol) was obtained as an amorphous powder after further drying under high vacuum. (Yield: 0.9 %)

**<sup>1</sup>H NMR (400 MHz, DMSO-*d*<sub>6</sub>)** δ 6.20 (d, *J* = 9.3 Hz, 1H) 7.37 (s, 1H), 7.36 (s, 1H), 7.42 (d, *J* = 9.3 Hz, 1H), 8.00 (s, 1H), 8.36 (s, 1H), 9.21 (s, 1H), 10.78 (s, 1H). **<sup>13</sup>C NMR (101 MHz, DMSO-*d*<sub>6</sub>)** δ 50.6, 102.9, 105.8, 116.6, 120.0, 129.7, 138.4, 143.7, 150.2, 167.4, 174.7, 178.3. *t*<sub>R</sub> 1.77 min, UPLC (ESI) *m/z* 248.0 [M+H]<sup>+</sup> (92 %)

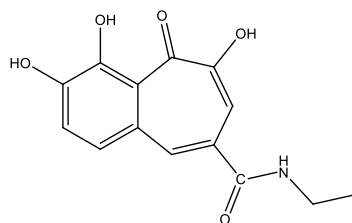
### 3,4,6-Trihydroxy-*N*-methyl-5-oxo-5H-benzo[7]annulene-8-carboxamide (22)



Following **general procedure C**, *N*-Methyl-3,4,5-trihydroxybenzamide **5b** (0.460 g, 2.51 mmol) and pyrocatechol (0.277 g, 2.51 mmol) were used. After extra washing steps with small volumes of water, the compound was further dried under high vacuum to give the desired 3,4,6-Trihydroxy-*N*-methyl-5-oxo-5H-benzo[7]annulene-8-carboxamide (0.540 g, 2.067 mmol) as an amorphous powder. (Yield: 82 %)

**<sup>1</sup>H NMR (400 MHz, DMSO-*d*<sub>6</sub>)** δ 2.79 (d, *J* = 4.5 Hz, 3H), 7.50 (d, *J* = 4.7 Hz, 1H), 7.53 (s, 1H), 7.99 (s, 1H), 8.59 (d, *J* = 4.6 Hz, 1H), 9.64 (s, 1H), 10.18 (s, 1H), 14.80 (s, 1H). **<sup>13</sup>C NMR (101 MHz, DMSO-*d*<sub>6</sub>)** δ 26.4, 115.7, 121.9, 126.7, 128.2, 129.1, 134.7, 138.4, 146.9, 150.8, 153.4, 167.5, 184.5. *t*<sub>R</sub> 2.10 min, UPLC (ESI) *m/z* 262.1 [M+H]<sup>+</sup> (91 %)

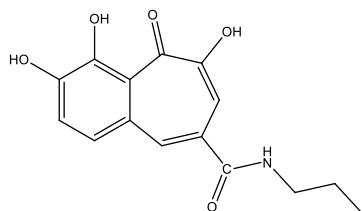
### *N*-Ethyl-3,4,6-trihydroxy-5-oxo-5H-benzo[7]annulene-8-carboxamide (23)



Following **general procedure C**, *N*-Ethyl-3,4,5-trihydroxybenzamide **5c** (0.230 g, 1.166 mmol) and pyrocatechol (0.128 g, 1.166 mmol) were used. The desired *N*-Ethyl-3,4,6-trihydroxy-5-oxo-5H-benzo[7]annulene-8-carboxamide (0.085 g, 0.309 mmol) was obtained as an amorphous powder. (Yield: 27 %)

**<sup>1</sup>H NMR (400 MHz, DMSO-*d*<sub>6</sub>)** δ 1.14 (t, *J* = 7.2 Hz, 3H), 3.27 (p, *J* = 7.3 Hz, 2H), 7.48 (d, *J* = 8.6 Hz, 1H), 7.51 (s, 1H), 7.54 (s, 1H), 7.99 (s, 1H), 8.63 (t, *J* = 5.3 Hz, 1H), 9.65 (s, 1H), 10.19 (s, 1H), 14.82 (s, 1H). **<sup>13</sup>C NMR (101 MHz, DMSO-*d*<sub>6</sub>)** δ 14.6, 34.6, 116.5, 120.2, 122.2, 127.1, 128.4, 129.4, 135.0, 147.5, 150.8, 153.4, 166.9, 184.5. *t*<sub>R</sub> 1.31 min, UPLC (ESI) *m/z* 276.0 [M+H]<sup>+</sup> (100 %)

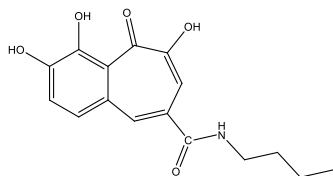
### 3,4,6-Trihydroxy-5-oxo-*N*-propyl-5*H*-benzo[7]annulene-8-carboxamide (24)



Following **general procedure C**, *N*-Propyl-3,4,5-trihydroxybenzamide **5d** (0.250 g, 1.184 mmol) and pyrocatechol (0.130 g, 1.184 mmol) were used. The desired 3,4,6-Trihydroxy-5-oxo-*N*-propyl-5*H*-benzo[7]annulene-8-carboxamide (0.187 g, 0.645 mmol) was obtained as an amorphous powder. (Yield: 55 %)

**<sup>1</sup>H NMR (400 MHz, DMSO-*d*<sub>6</sub>)** δ 0.91 (t, *J* = 7.4 Hz, 3H), 1.52 (sx, *J* = 7.5 Hz, 2H), 3.22 (q, *J* = 6.8 Hz, 2H), 7.49 (t, *J* = 8.2 Hz, 2H), 7.53 (s, 1H), 7.98 (s, 1H), 8.61 (t, *J* = 5.5 Hz, 1H), 9.64 (s, 1H), 10.17 (s, 1H), 14.81 (s, 1H). **<sup>13</sup>C NMR (101 MHz, DMSO-*d*<sub>6</sub>)** δ 11.5, 22.2, 41.5, 116.5, 120.1, 122.1, 127.0, 128.5, 129.4, 135.0, 147.5, 150.8, 153.3, 167.1, 184.5. *t*<sub>R</sub> 1.41 min, UPLC (ESI) *m/z* 290.1 [M+H]<sup>+</sup> (100 %).

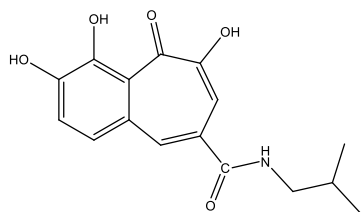
### *N*-Butyl-3,4,6-trihydroxy-5-oxo-5*H*-benzo[7]annulene-8-carboxamide (25)



Following **general procedure C**, *N*-Butyl-3,4,5-trihydroxybenzamide **5e** (1.230 g, 5.46 mmol) and pyrocatechol (0.601 g, 5.46 mmol) were used. After additional washing steps with small volumes of water, the desired *N*-Butyl-3,4,6-trihydroxy-5-oxo-5*H*-benzo[7]annulene-8-carboxamide (0.997 g, 3.29 mmol) was obtained as an amorphous powder. (Yield: 60 %)

**<sup>1</sup>H NMR (400 MHz, DMSO-*d*<sub>6</sub>)** δ 0.89 (t, *J* = 7.3 Hz, 3H), 1.32 (sx, *J* = 7.3 Hz, 2H), 1.50 (p, *J* = 7.6 Hz, 2H), 3.24 (q, *J* = 6.8 Hz, 2H), 7.50 (m, 3H), 7.94 (s, 1H), 8.60 (t, *J* = 5.4 Hz, 1H), 9.67 (s, 1H), 10.27 (s, 1H), 14.75 (s, 1H). **<sup>13</sup>C NMR (101 MHz, DMSO-*d*<sub>6</sub>)** δ 13.9, 19.8, 31.2, 116.6, 120.3, 122.4, 127.3, 128.7, 129.6, 135.2, 147.7, 150.9, 153.5, 167.5, 184.7. *t*<sub>R</sub> 1.59 min, UPLC (ESI) *m/z* 302.5 [M-H]<sup>-</sup> (100 %)

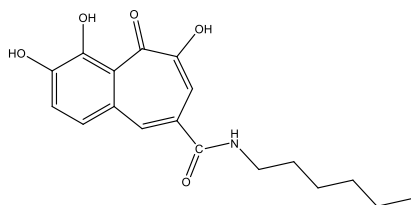
### 3,4,6-Trihydroxy-*N*-isobutyl-5-oxo-5*H*-benzo[7]annulene-8-carboxamide (26)



Following **general procedure C**, 3,4,5-Trihydroxy-*N*-isobutylbenzamide **5f** (0.42 g, 1.865 mmol) and pyrocatechol (0.205 g, 1.865 mmol) were used. The desired 3,4,6-Trihydroxy-*N*-isobutyl-5-oxo-5*H*-benzo[7]annulene-8-carboxamide (0.056 g, 0.185 mmol) was obtained as an amorphous powder. (Yield: 10 %)

**<sup>1</sup>H NMR (400 MHz, DMSO-*d*<sub>6</sub>)** δ 0.91 (d, *J* = 6.7 Hz, 6H) 1.85 (sx, *J* = 6.7 Hz, 1H), 3.08 (t, *J* = 6.8 Hz, 2H), 7.51 (m, 3H), 7.98 (s, 1H), 8.62 (t, *J* = 5.7 Hz, 1H), 9.64 (s, 1H), 10.17 (s, 1H), 14.81 (s, 1H). **<sup>13</sup>C NMR (101 MHz, DMSO-*d*<sub>6</sub>)** δ 20.2, 28.0, 47.2, 116.5, 120.1, 122.1, 127.1, 128.5, 129.4, 135.0, 147.5, 150.8, 153.3, 167.3, 184.5. *t*<sub>R</sub> 1.65 min, UPLC (ESI) *m/z* 302.1 [M-H]<sup>-</sup> (100 %)

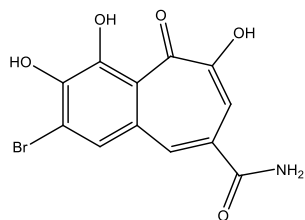
### *N*-Hexyl-3,4,6-trihydroxy-5-oxo-5*H*-benzo[7]annulene-8-carboxamide (27)



Following **general procedure C**, *N*-Hexyl-3,4,5-trihydroxybenzamide **5g** (1.450 g, 5.72 mmol) and pyrocatechol (0.630 g, 5.72 mmol) were used. After additional washing steps with small volumes of water, the desired *N*-Hexyl-3,4,6-trihydroxy-5-oxo-5*H*-benzo[7]annulene-8-carboxamide (1.220 g, 3.680 mmol) was obtained as an amorphous powder. (Yield: 64 %)

**<sup>1</sup>H NMR (400 MHz, DMSO-*d*<sub>6</sub>)** δ 0.87 (t, *J* = 6.6 Hz, 3H), 1.26 (m, 6H), 1.51 (p, *J* = 7.0 Hz, 2H), 3.24 (q, *J* = 6.8 Hz, 2H), 7.47- 7.50 (m, 3H), 7.97 (s, 1H), 8.60 (t, *J* = 5.4 Hz, 1H), 9.65 (s, 1H), 10.20 (s, 1H), 14.80 (s, 1H). **<sup>13</sup>C NMR (101 MHz, DMSO-*d*<sub>6</sub>)** δ 13.9, 22.1, 26.2, 28.9, 31.0, 116.5, 120.2, 122.2, 127.1, 128.5, 129.4, 135.0, 147.5, 150.8, 153.4, 167.1, 184.5. *t*<sub>R</sub> 1.88 min, UPLC (ESI) *m/z* 330.5 [M-H]<sup>-</sup> (100 %)

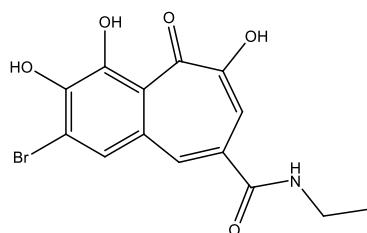
### 2-Bromo-3,4,6-trihydroxy-5-oxo-5H-benzo[7]annulene-8-carboxamide (28)



Following **general procedure C**, 3,4,5-Trihydroxybenzamide **5a** (0.483 g, 2.86 mmol) and 3-bromobenzene-1,2-diol (0.540g, 2.86 mmol) were used. The obtained precipitate was suspended in methanol and filtered. The filtrate was evaporated to give the desired 2-Bromo-3,4,6-trihydroxy-5-oxo-5H-benzo[7]annulene-8-carboxamide (0.798 g, 2.447 mmol) as a pure powder. (Yield: 85 %)

**<sup>1</sup>H NMR (400 MHz, DMSO-*d*<sub>6</sub>)**  $\delta$  7.55 (s, 1H), 7.60 (s, 1H), 7.87 (s, 1H), 8.05 (brs, 2H), 9.81 (s, 1H), 10.74 (s, 1H), 15.32 (s, 1H). **<sup>13</sup>C NMR (101 MHz, DMSO-*d*<sub>6</sub>)**  $\delta$  116.6, 116.8, 119.2, 128.8, 129.2, 129.7, 134.1, 144.6, 151.3, 153.9, 168.5, 184.3.  $t_R$ : 1.21, UPLC (ESI)  $m/z$  324.3/326.3 (1:1) [M-H]<sup>-</sup> (100 %)

### 2-Bromo-N-ethyl-3,4,6-trihydroxy-5-oxo-5H-benzo[7]annulene-8-carboxamide (29)

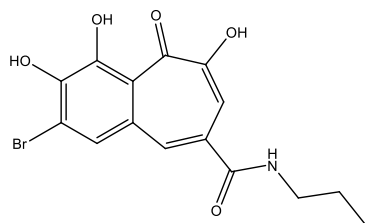


Following **general procedure C**, N-Ethyl-3,4,5-trihydroxybenzamide **5c** (0.270 g, 1.369 mmol) and 3-bromobenzene-1,2-diol (0.259 g, 1.369 mmol) were used. The desired 2-Bromo-N-ethyl-3,4,6-trihydroxy-5-oxo-5H-benzo[7]annulene-8-carboxamide (0.302 g, 0.853 mmol) was obtained as an amorphous powder. (Yield: 62 %).

**<sup>1</sup>H NMR (400 MHz, DMSO-*d*<sub>6</sub>)**  $\delta$  1.13 (t,  $J$  = 7.3 Hz, 3H), 3.29 (q,  $J$  = 7.2 Hz, 2H), 7.52 (s, 1H), 7.89 (s, 1H), 7.95 (s, 1H), 8.59 (t,  $J$  = 5.3 Hz, 1H), 9.86 (s, 1H), 10.76 (s, 1H), 15.31 (s, 1H). **<sup>13</sup>C NMR (101 MHz, DMSO-*d*<sub>6</sub>)**  $\delta$  14.5, 34.6, 116.6, 116.8, 119.0, 128.7, 129.7, 129.8, 133.6, 144.5, 151.2, 154.0, 166.7, 184.3.  $t_R$  1.48 min, UPLC (ESI)  $m/z$  352.0/354.0 (1:1) [M-H]<sup>-</sup> (100 %)



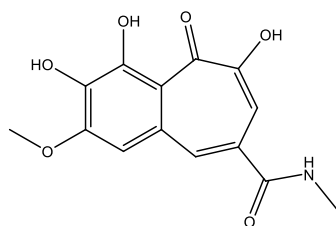
### 2-Bromo-3,4,6-trihydroxy-5-oxo-*N*-propyl-5*H*-benzo[7]annulene-8-carboxamide (30)



Following **general procedure C**, 3,4,5-Trihydroxy-*N*-propylbenzamide **5d** (0.240 g, 1.136 mmol) and 3-bromobenzene-1,2-diol (0.215 g, 1.136 mmol) were used. The desired 2-Bromo-3,4,6-trihydroxy-5-oxo-*N*-propyl-5*H*-benzo[7]annulene-8-carboxamide (0.263 g, 0.714 mmol) was obtained as an amorphous powder. (Yield: 63 %)

**<sup>1</sup>H NMR (400 MHz, DMSO-*d*<sub>6</sub>)** δ 0.91 (t, *J* = 7.4 Hz, 3H), 1.54 (sx, *J* = 7.2 Hz, 2H), 3.22 (q, *J* = 6.8 Hz, 2H), 7.53 (s, 1H), 7.95 (s, 1H), 7.89 (s, 1H), 8.57 (t, *J* = 5.5 Hz, 1H), 9.84 (s, 1H), 10.72 (s, 1H), 15.31 (s, 1H). **<sup>13</sup>C NMR (101 MHz, DMSO-*d*<sub>6</sub>)** δ 11.5, 22.2, 41.5, 116.6, 116.8, 119.0, 128.7, 129.7, 129.9, 133.6, 144.1, 150.8, 154.0, 166.9, 184.3. *t*<sub>R</sub> 1.62 min, UPLC (ESI) *m/z* 368.0/370.0 (1:1) [M] (95 %)

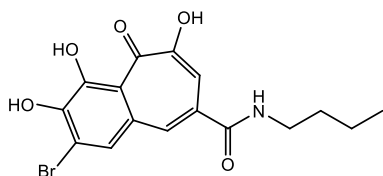
### 3,4,6-Trihydroxy-2-methoxy-*N*-methyl-5-oxo-5*H*-benzo[7]annulene-8-carboxamide (31)



Following **general procedure C**, 3,4,5-Trihydroxy-*N*-methylbenzamide **5b** (0.400 g, 2.184 mmol) and 3-methoxybenzene-1,2-diol (0.306 g, 2.184 mmol) were used, but no precipitate was formed. Instead, the filtrate was extracted with 3 x 20 mL EtOAc and residual water was removed by addition of Na<sub>2</sub>SO<sub>4</sub>. After evaporation of EtOAc, the obtained product was washed several times with small amounts of 1M HCl to remove minor impurities. The desired 3,4,6-Trihydroxy-2-methoxy-*N*-methyl-5-oxo-5*H*-benzo[7]annulene-8-carboxamide (0.358 g, 1.229 mmol) was obtained as an amorphous powder. (Yield: 56 %)

**<sup>1</sup>H NMR (400 MHz, DMSO-*d*<sub>6</sub>)** δ 2.79 (d, *J* = 4.5 Hz, 3H), 3.99 (s, 3H), 7.28 (s, 1H), 7.47 (s, 1H), 8.04 (s, 1H), 8.58 (s, 1H), 9.61 (s, 1H), 14.96 (s, 1H). **<sup>13</sup>C NMR (101 MHz, DMSO-*d*<sub>6</sub>)** δ 26.7, 56.0, 108.5, 115.0, 116.1, 128.6, 130.8, 134.3, 136.6, 151.0, 152.1, 153.9, 167.7, 182.6. *t*<sub>R</sub> 1.25 min, UPLC (ESI) *m/z* 290.5 [M-H]<sup>-</sup> (100 %)

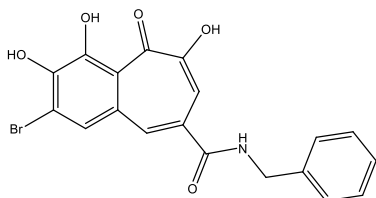
### 2-Bromo-*N*-butyl-3,4,6-trihydroxy-5-oxo-5*H*-benzo[7]annulene-8-carboxamide (32)



Following **general procedure C**, *N*-Butyl-3,4,5-trihydroxybenzamide **5e** (0.238 g, 1.058 mmol) and 3-bromobenzene-1,2-diol (0.200 g, 1.058 mmol) were used. The desired 2-Bromo-*N*-butyl-3,4,6-trihydroxy-5-oxo-5*H*-benzo[7]annulene-8-carboxamide (0.174 g, 0.455 mmol) was obtained as an amorphous powder. (Yield: 43 %)

**<sup>1</sup>H NMR (400 MHz, DMSO-*d*<sub>6</sub>)** δ 0.91 (t, *J* = 7.3 Hz, 3H), 1.36 (sx, *J* = 7.2 Hz, 2H), 1.47 - 1.56 (m, 2H), 3.25 (q, *J* = 6.9 Hz, 2H), 7.52 (s, 1H), 7.89 (s, 1H), 7.94 (s, 1H), 8.56 (t, *J* = 5.5 Hz, 1H), 9.85 (s, 1H), 10.74 (s, 1H), 15.32 (s, 1H). **<sup>13</sup>C NMR (101 MHz, DMSO-*d*<sub>6</sub>)** δ 13.7, 19.6, 31.0, 116.6, 116.8, 118.9, 128.7, 129.7, 129.9, 133.6, 144.5, 151.2, 154.0, 166.8, 184.3. *t*<sub>R</sub> 1.74 min, UPLC (ESI) *m/z* 382.0/384.0 (1:1) [M] (100 %)

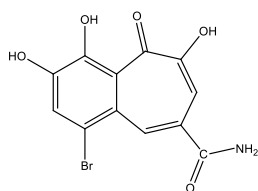
### *N*-Benzyl-2-bromo-3,4,6-trihydroxy-5-oxo-5*H*-benzo[7]annulene-8-carboxamide (33)



Following **general procedure C**, *N*-Benzyl-3,4,5-trihydroxybenzamide **5e** (0.274g, 1.058 mmol) and 3-bromobenzene-1,2-diol (0.200 g, 1.058 mmol) were used. The desired *N*-Benzyl-2-bromo-3,4,6-trihydroxy-5-oxo-5*H*-benzo[7]annulene-8-carboxamide (0.312 g, 0.750 mmol) was obtained as an amorphous powder. (Yield: 71 %)

**<sup>1</sup>H NMR (400 MHz, DMSO-*d*<sub>6</sub>)** δ 4.48 (s, 2H), 7.35 (m, 5H), 7.57 (s, 1H), 7.90 (s, 1H), 8.04 (s, 1H), 9.16 (s, 1H), 9.88 (s, 1H), 10.77 (s, 1H), 15.32 (s, 1H). **<sup>13</sup>C NMR (101 MHz, DMSO-*d*<sub>6</sub>)** δ 43.2, 116.5, 116.6, 118.7, 126.8, 127.3, 128.3, 128.7, 129.3, 129.5, 133.8, 139.2, 144.3, 150.8, 154.0, 166.9, 183.5. *t*<sub>R</sub> 1.76 min, UPLC (ESI) *m/z* 416.1/418.1 (1:1) [M] (100 %)

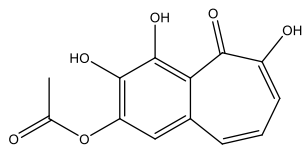
### 2-Bromo-3,4,6-trihydroxy-5-oxo-5H-benzo[7]annulene-8-carboxamide (34)



Following **general procedure C**, 3,4,5-Trihydroxybenzamide **5a** (0.483 g, 2.86 mmol) and 3-bromobenzene-1,2-diol (0.540g, 2.86 mmol) were used. The obtained precipitate was suspended in methanol and filtered. The filtrate was evaporated to give the desired 2-Bromo-3,4,6-trihydroxy-5-oxo-5H-benzo[7]annulene-8-carboxamide (0.789 g, 2.420 mmol) as an amorphous powder. (Yield: 85 %)

**<sup>1</sup>H NMR (400 MHz, DMSO-*d*<sub>6</sub>)** δ 7.55 (s, 1H), 7.60 (s, 1H), 7.87 (s, 1H), 8.05 (brs, 2H), 9.81 (s, 1H), 10.74 (s, 1H), 15.32 (s, 1H). **<sup>13</sup>C NMR (101 MHz, DMSO-*d*<sub>6</sub>)** δ 116.6, 116.8, 119.2, 128.8, 129.2, 129.7, 134.1, 144.6, 151.3, 153.9, 168.5, 184.3. *t*<sub>R</sub> 1.21 min, UPLC (ESI) *m/z* 324.3/326.3 (1:1) [M-H]<sup>-</sup> (100 %)

### 3,4,6-Trihydroxy-5-oxo-5H-benzo[7]annulene-2-yl acetate (36)



To a stirred solution of 2,3,4,6-Tetrahydroxy-5H-benzo[7]annulene-5-one **35** (0.120 g, 0.545 mmol) in 6 mL of pyridine were slowly added 3 eq. of acetic anhydride over 30 min at 110°C. After stirring for 12 h, 20 mL 1M HCl was added, and the reaction mixture was extracted with 3 x 15 mL DCM. The organic phases were combined and dried over Na<sub>2</sub>SO<sub>4</sub>. Afterwards, the organic phase was evaporated using a rotary evaporator to give a yellow solid. The obtained product was further purified by flash chromatography on silica gel, using EtOAc/hexane (1:1) as eluent, to afford the desired 3,4,6-Trihydroxy-5-oxo-5H-benzo[7]annulene-2-yl acetate (0.021 g, 0.080 mmol) as an amorphous powder. (Yield: 15 %) [5]

**<sup>1</sup>H NMR (400 MHz, DMSO-*d*<sub>6</sub>)** δ 2.32 (s, 3H), 6.84 (d, *J* = 10.6 Hz, 1H), 6.88 (s, 1H), 7.05 (d, *J* = 9.3 Hz, 1H), 7.34 (d, *J* = 11.5 Hz, 1H), 9.68 (s, 1H), 11.23 (s, 1H), 15.51 (s, 1H). **<sup>13</sup>C NMR (101 MHz, DMSO-*d*<sub>6</sub>)** δ 20.3, 109.6, 114.3, 116.3, 126.5, 133.6, 138.4, 155.2, 155.9, 157.7, 168.0, 183.1. *t*<sub>R</sub> 1.55 min, UPLC (ESI) *m/z* 261.4 [M-H]<sup>-</sup> (94 %)

## **1.2. Biochemistry**

### **1.2.1 Screening protocols**

#### **1.2.1.1 SDS-PAGE-based screening assay for Atg4B inhibition**

##### **1.2.1.1.1 Substrate and enzyme origin**

The LC3B-GST coding sequence was inserted into the pET11a vector (Novagen), and expressed in *Escherichia Coli*. The recombinant HsAtg4B enzyme was produced in *Escherichia Coli* as GST-HsAtg4B and purified by GST-affinity chromatography. The GST tag was removed with PreScission protease. Enzyme purification was performed as described by Sugawara et al [6].

##### **1.2.1.1.2 General SDS-PAGE assay procedure**

LC3B-GST (2 µg/µL) dissolved in 50 mM Tris pH 8.0, 150 mM NaCl and 1 mM DTT and HsAtg4B (2.34 µg/µL) dissolved in 20 mM Tris pH 7.4, 150 mM NaCl and 2 mM DTT were stored in a -80 °C freezer in small aliquots. For each assay, fresh aliquots of enzyme and substrate were thawed, and fresh buffer was used. All substrate and enzyme dilutions were made in LoBind Eppendorf® tubes. Buffer used in the following methods for making appropriate dilutions consisted of 50 mM Tris-HCl pH 7.4, 150 mM NaCl, 2 mM DTT and 0.1% TWEEN 20, freshly prepared at the day of the experiment. 10 µL of Laemmli Sample Buffer was added to each sample to stop enzymatic cleavage of LC3B-GST and the samples were boiled for 4 minutes. The samples were loaded onto a NuPAGE® Novex 12 Bis-Tris 1.0 mm 15 well gel after termination of the enzymatic reaction. A Thermo-Scientific® PageRuler Prestained Protein Ladder was used as a reference for molecular weights of the separated proteins. Gels were run in a NuPAGE Bolt® Mini Gel Tank for 50 minutes using NuPAGE® MOPS SDS Running Buffer at constant voltage (170V) using a Bio-Rad PowerPac® Basic 300 V Power Supply. Gels were stained for 2 hours using Oriole™ Fluorescent Gel Stain, (purchased from Bio-Rad®), and destained by washing several times with Milli-Q™ water. Lane densities were scanned using a Roche® Lumi-Imager® F1 at a UV max of 600 nm and an exposure time of 500 ms, yielding three clearly visible bands per lane (from top to bottom): uncleaved LC3B-GST, free GST and free LC3B. Lane densities were quantified using Totallab Quant® software.

### 1.2.1.1.3 Protocol for determination of Atg4B inhibition using the SDS-PAGE-based screening assay

Compounds were dissolved in DMSO in a 10 mM concentration (final concentration of 500  $\mu$ M in the assay). Fivefold dilutions of the library compounds were made in buffer. Atg4B and LC3B-GST aliquots were thawed and dilutions were made (Atg4B: 0.625 ng/ $\mu$ L; LC3B-GST: 0.4  $\mu$ g/ $\mu$ L). To 2.5  $\mu$ L of LC3B-GST was added 2.5  $\mu$ L of testing compound. Per gel a maximum of 13 compounds was loaded. A control sample was made consisting of 2.5  $\mu$ L of substrate dilution and 2.5  $\mu$ L of buffer solution containing 20 % v/v of DMSO (5 % in the final mixture). 5  $\mu$ L of Atg4B was added to each one of the 14 samples and incubated at room temperature for 6 minutes. Reactions were stopped by adding Laemmli sample buffer. Eventually, quantification of both the intact fusion protein and its cleavage products was performed using optical densitometry. The percentage of uncleaved [LC3B-GST] was used as a measure for Atg4B activity, and was calculated using the following formula (OD= Optical Density):

$$\% \text{ uncleaved [LC3B - GST]} = \frac{OD([LC3B-GST])}{OD([LC3B-GST]) + OD(GST) + OD(LC3B)} \times 100\%$$

The percentage of uncleaved substrate was then used to express the amount of enzyme inhibition as percent inhibition. Herefore, we set the percentage of uncleaved substrate in the control sample as zero percent of inhibition, while 100% of uncleaved substrate corresponded to complete enzyme inhibition. For this conversion, we applied the following formula:

$$\text{enzyme inh. (\%)} = \frac{\text{uncleaved}([LC3B-GST])_{\text{test sample}} - \text{uncleaved}([LC3B-GST])_{\text{control sample}}}{100 - \text{uncleaved}([LC3B-GST])_{\text{control sample}}} \times 100\%$$

In case of a negative percent inhibition (suggesting Atg4B induction), the outcome was set to zero percent.

### **1.2.1.2 CYTO-ID-based phenotypical screening for autophagy inhibition**

Compounds were obtained as a 10 mM stock dissolved in 100% DMSO (Acros Organics, 167850010). Jurkat T-cells were cultured in RPMI 1640 medium (Invitrogen, San Diego, California) supplemented with 10% fetal bovine serum. A total of  $1 \times 10^6$  cells was transferred into a standard 12-well plate. Cells were treated with 10  $\mu$ M everolimus (Novartis Institutes for Biomedical Research, Basel, Switzerland) dissolved in 100% EtOH in the presence of 10  $\mu$ M of the compound to be tested. A set of controls were incorporated into the experiments: untreated Jurkat T-cells, cells treated with 10  $\mu$ M everolimus and cells treated with both 10  $\mu$ M everolimus and 10 mM 3-MA. Following 16 hours of treatment, cells were washed and autophagosomes were stained for 30 minutes with CYTO-ID Green Autophagy Detection Reagent (Enzo Life Sciences Inc., ENZ-51031-K200) according to manufacturer's protocol. Cells were then washed and passed through a flow cytometer (Accuri c6, BD biosciences) to count individual Jurkat T-cells which incorporated the fluorescent CYTO-ID dye.

### **1.2.1.3 Luciferase reporter assay for assessment of intracellular Atg4B inhibition**

#### **1.2.1.3.1 Plasmid transformation and purification**

A pEAK12 plasmid bearing the sequence for a Gaussia luciferase (GLUC) reporter fused to the ATG4 substrate LC3 and ankered in the cell with  $\beta$ -actin ( $\beta$ -actin-LC3-GLUC) was obtained from Dr. Ketteler (R. MRC Laboratory for molecular cell biology, UCL, London, UK). The plasmid was transformed into *E. coli* (One Shot® TOP10 kit, invitrogen, C4040-03) according to standard procedures. After allowing to grow, purification of the plasmid out of a 1 liter culture was performed using Plasmid Maxi kit (Qiagen, 12162).

#### **1.2.1.3.2 Transfection**

HEK 293T cells were cultured in DMEM medium (Invitrogen, San Diego, California) supplemented with 10 % fetal bovine serum. Amaxa Cell Line Nucleofector kit V (Lonza, VCA-1003, USA) was used to transfect  $2 \times 10^6$  cells with either 3  $\mu$ g of the purified pEAK12 plasmid or control plasmid (pmaxGFP®) according to standard procedures. Cells were then transferred to a 24-well plate and incubated at 37 °C.

### 1.2.1.3.3 Screening protocol for in cellulo Atg4B inhibition

24 hours post transfection, medium in which HEK 293T cells were cultured was removed and 500  $\mu$ L fresh serum free RPMI medium was added. The medium contained no treatment, 10  $\mu$ M everolimus or everolimus + 10  $\mu$ M of the compound to be tested. Cells were incubated for 6 hours after which medium was removed for analysis. BioLux Gaussia Luciferase Assay kit (NEB, E3300S, UK) was used to measure the luciferase activity. Briefly, 10  $\mu$ L of the medium was transferred in an opaque 96-well microtiter plate and mixed with 50  $\mu$ L assay buffer. The luciferase activity was measured after a 5 seconds integration time using the Infinite® 200 Pro microplate reader (Tecan).

### References

- [1] G. D. Thorn, L. R. C. Barclay; *Can. J. Chem.* 30 (1952), 251-256.
- [2] A. Kurdi, M. Cleenewerck, C. Vangestel, S. Lyssens, W. Declercq, J.P. Timmermans, S. Stroobants, K. Augustyns, G. R.Y. De Meyer, P. V. Der Veken, W. Martinet; *Biochem. Pharmacol.* 138 (2017), 150-162.
- [3] K. Dodoab, T. Minatoa, T. Noguchi-Yachidea, M. Suganumac, Y. Hashimotoa; *Bioorg. Med. Chem.* 16 (2008), 7975-7982
- [4] Ozinsky, A.; Underhill, D. M.; Fontenot, J. D.; Hajjar, A. M.; Smith, K. D.; Wilson, C. B.; Schroeder, L.; Aderem. *Proc. Natl. Acad. Sci. USA.* (2000), 97, 13766-13771.
- [5] Zou, H. B.; Dong, S. Y.; Zhou, C. X.; Hu, L. H.; Wu, Y. H.; Li, H. B.; Gong, J. X.; Sun, L. L.; Wu, M. X.; Bai, H.; Fan, B. T.; Hao, X. J.; Stöckigt, J.; Zhao, Y. *Bioorganic Med. Chem.* (2006), 14, 2060-2071.
- [6] K. Sugawara; N.N. Suzuki; Y. Fujioka; N. Mizushima; Y. Ohsumi; F. Inagaki; *J. Biol. Chem.* 280 (2005), 40058-40065.